Electronic Supporting Information

Pyridine coupled mono and bisbenzimidazoles as supramolecular gelators: Selective metal ion sensing and ion conductivity

Santanu Panja,[a] Subhratanu Bhattacharya,[b] Kumaresh Ghosh[a]*

[a]*Department of Chemistry, University of Kalyani, Kalyani-741235, India, Email: ghosh_k2003@yahoo.co.in*

[a]*Department of Physics, University of Kalyani, Kalyani-741235, India.*

Table of contents

Table 1S. Results of gelation test for **1-6**.

Solvent	**1**	**2**	**3**	**4**	**5**	**6**
$CHCl_3$	I	PS	I	S	I	PS
DCM	I	I	I	S	I	I
$CHCl_3$: MeOH (100:2,v/v)	I	S	PS	S	I	S
$CHCl_3$: MeOH (1:1,v/v)	S	S	S	S	S	S
MeOH	S	S	S	S	S	S
Acetonitrile	I	PS	I	PS	I	I
n-Hexane	I	I	I	I	I	I
Diethyl ether	I	I	I	I	I	I
Cyclohexane	I	I	I	I	I	I
Ethylacetate	PS	S	S	S	S	S
THF	PS	S	S	S	S	S
DMF	S	S	S	S	S	S
DMSO	S	S	S	S	S	S
THF: H_2O (1:1 , v/v)	P	S	P	S	P	S
DMF: H_2O (1:1 , v/v)	S	S	P	S	PG	S
MeOH: H_2O (1:1, v/v) + Ag^+	P	P	G	S	PG	P
MeOH: H_2O (1:2, v/v)	S	S	P	S	P	S
MeOH: H_2O (1:2, v/v) + Ag^+	P	P	P	G	P	P
MeOH: H_2O (1:3, v/v)	G	S	P	S	P	S
MeOH: H_2O (1:6, v/v)	P	G	P	P	P	P
DMSO: H_2O (1:1, v/v) + Ag^+	P	P	G	S	PG	P
DMSO: H_2O (1:2, v/v)	S	S	P	S	P	S
DMSO: H_2O (1:2, v/v) + Ag^+	P	P	P	G	P	P
DMSO: H_2O (1:3, v/v)	G	S	P	S	P	S
DMSO: H_2O (1:6, v/v)	P	G	P	P	P	P

S = solution; I = insoluble; G = gel (minimum gelatination concentration for **1** = 3.8 mg/mL, **2** = 5 mg/mL, **3** = 4.9 g/mL, **4** = 4.5 g/mL); P = precipitation; PS = partially soluble.

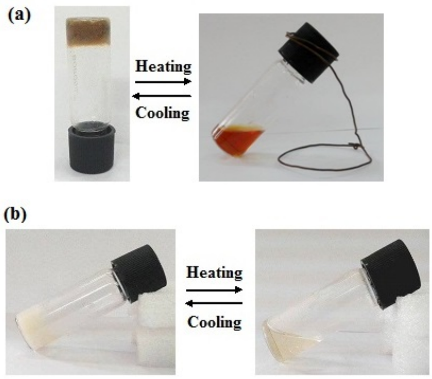

Fig. S1. Pictorial representation of the thermo reversibility of the DMSO: H_2O gels of (a) **1** and (b) **2**.

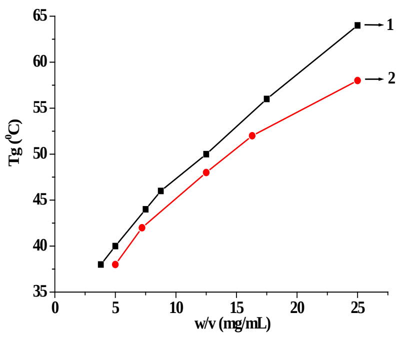

Fig. S2. Variation of gel melting temperature (Tg) with increasing concentration of gelators from DMSO: H_2O solvent system.

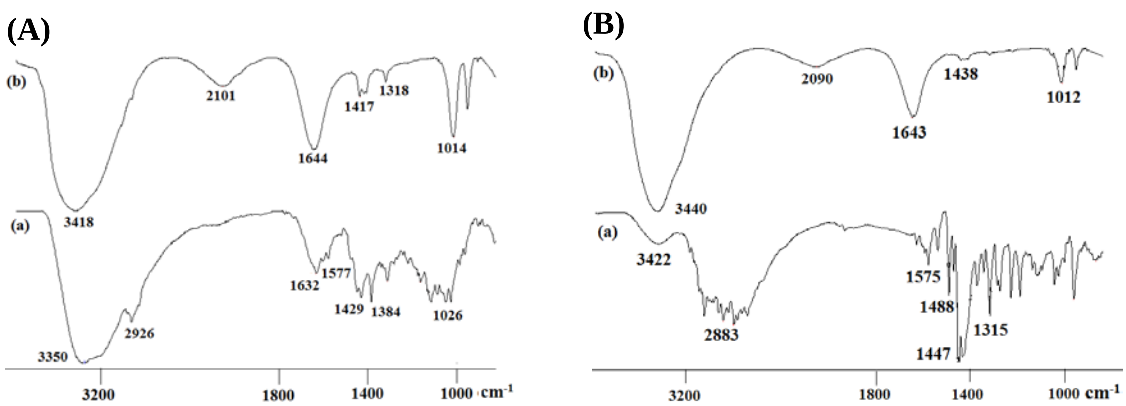

Fig. S3. Comparison of FTIR spectra of (A) **1** and (B) **2** in amorphous (a) and gel (b) states.

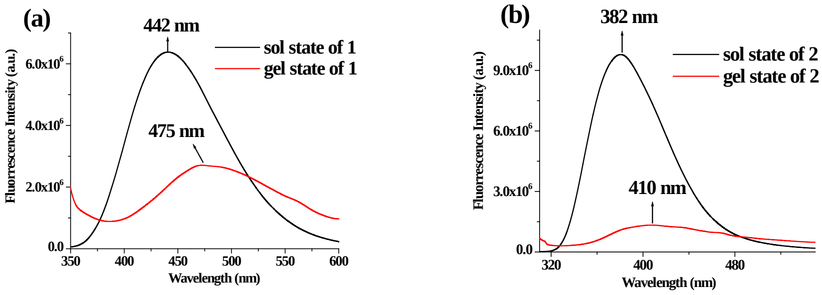

Fig. S4. Comparison of emission spectra of **1** (a) and **2** (b) in sol and gel states.

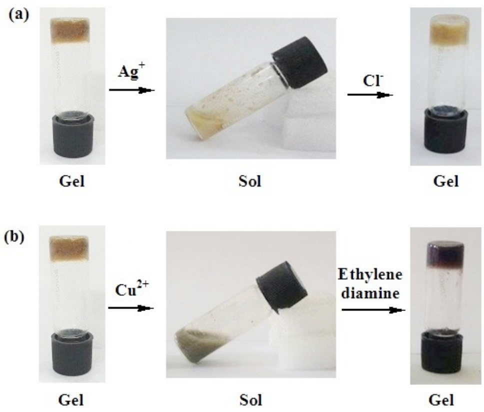

Fig. S5. Chemical responsiveness of the gel of **1** [8 mg/ mL in DMSO: H_2O (1:3, v/v)] on successive addition of (a) Ag^+ (c = 0.2 M) and Cl^- (b) Cu^{2+} (c = 0.2 M) and ethylene diamine.

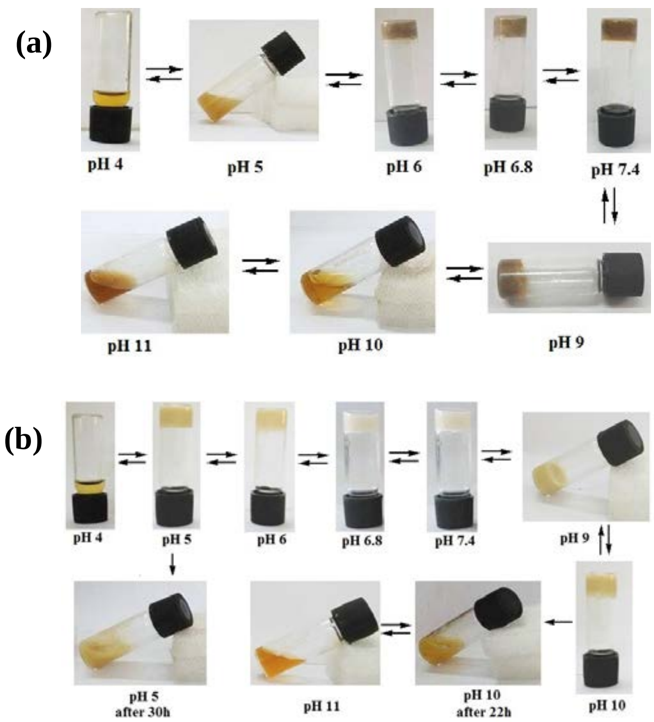

Fig. S6. Photograph showing the pH dependency of the DMSO: H_2O gels of **1** (a) and **2** (b).

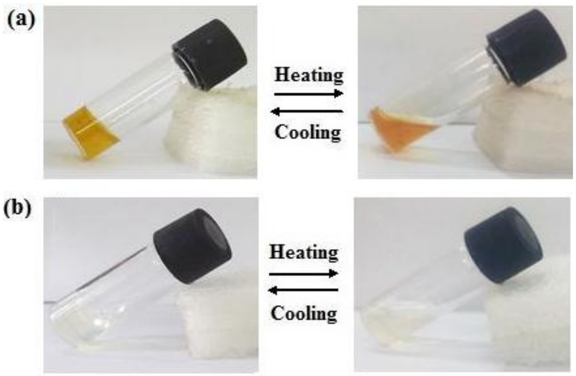

Fig. S7. Pictorial representation of thermo reversibility of the Ag^+-induced gel of (a) **3** and (b) **4** in DMSO: H_2O.

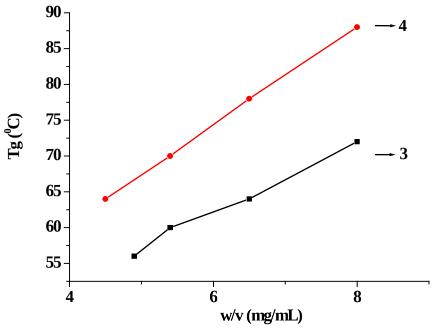

Fig. S8. Variation of gel melting temperature (T_g) with increasing concentration of gelators **3** and **4** in DMSO: H_2O solvent in presence of 2 equiv. amounts of Ag^+.

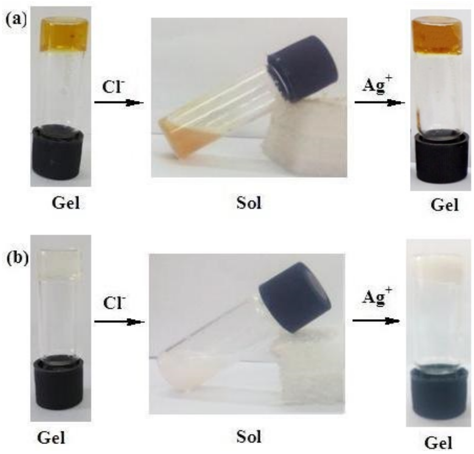

Fig. S9. Chemical responsiveness of the gels of (a) **3** [4.9 mg/ mL] and (b) **4** [4.5 mg/ mL] in DMSO: H_2O on successive addition of 2 equiv. amounts of Cl^- (c = 0.2 M) and Ag^+ (c = 0.2 M) ions, respectively. The Cl^--induced disrupted gel was recovered by adding Ag^+ solution after 4h and 2h for **3** and **4**, respectively.

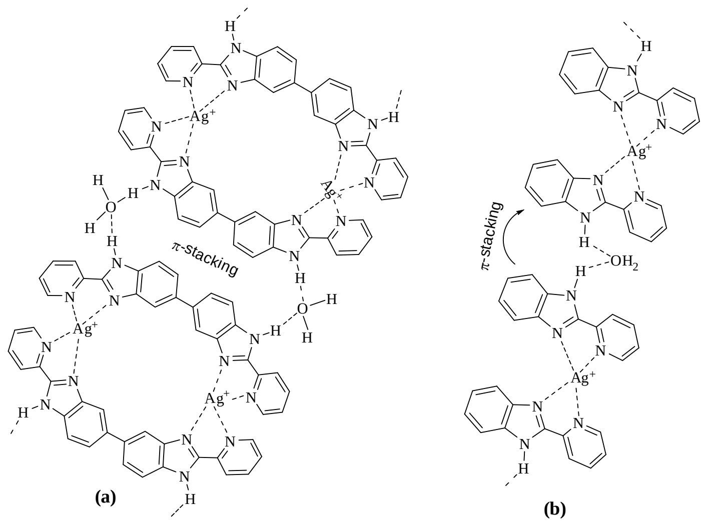

Fig. S10. Suggested modes of interaction of (a) **3** and (b) **4** involving Ag^{+} ions to form the networks responsible for gelation.

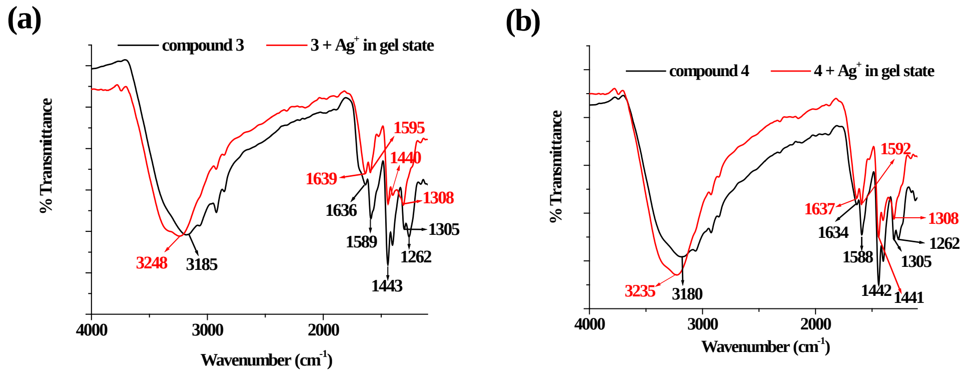

Fig. S11. FTIR spectra representing the change in stretching frequency in amorphous and gel states for (a) **3** and (b) **4**.

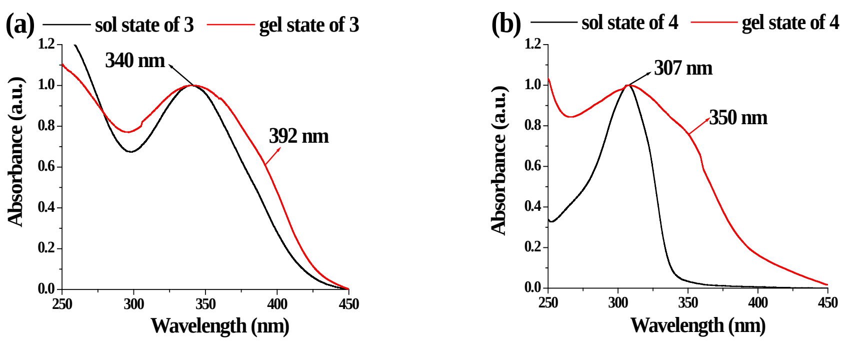

Fig. S12. Comparison of absorption spectra of **3** (a) and **4** (b) in the sol and gel states.

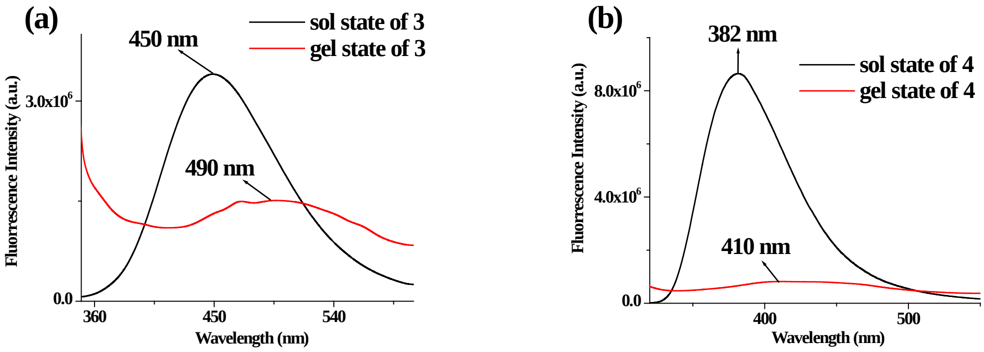

Fig. S13. Comparison of emission spectra of **3** (a) and **4** (b) in the sol and gel states.

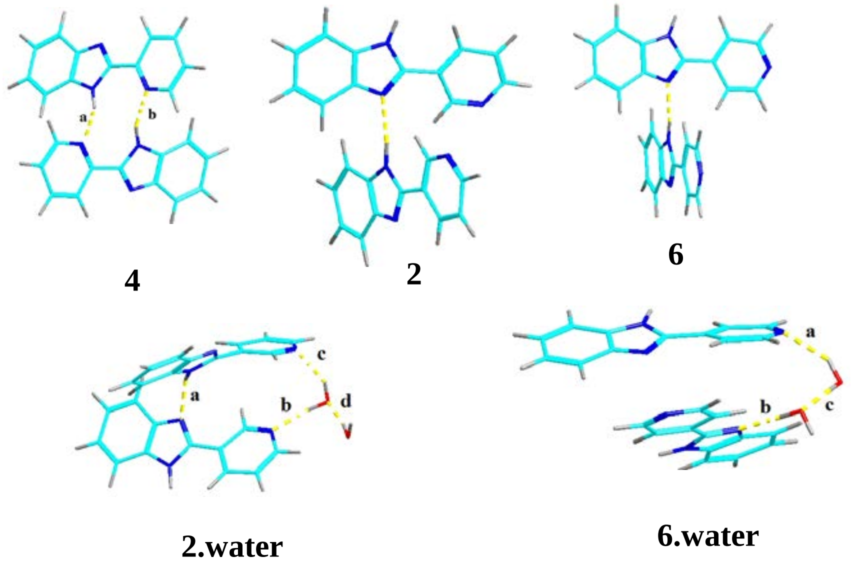

Fig. S14. MMX calculations: (A) Hydrogen bonded dimmers of **4** (E = 78.76 kcal/mol, a = b = 2.00Å), **2** (E = 62.90 kcal/mol; Hydrogen bond: distance: 2.19 Å) and **6** (E = 67.77 kcal/mol; Hydrogen bond distance: 1.97 Å); (B) water assembled dimmers of **2** (E = 49.12 kcal/mol; a = 2.08, b = 1.93, c = 1.97, d = 1.72; all are in Å) and **6** (E = 51.83 kcal/mol; a = 1.94, b = 1.82, c = 1.74; all are in Å) [Calculation was done using PC model, version 9.2, serena software].

Change in emission of 1 with metal ions

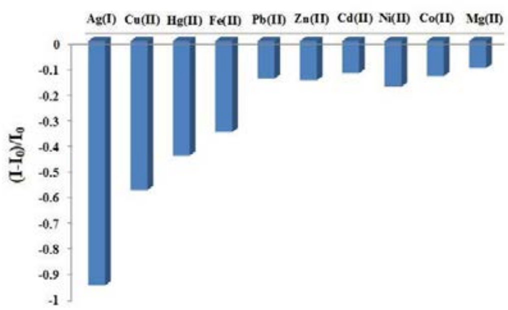

Fig. S15. Change in fluorescence ratio (λ_{ex} = 330 nm) of **1** (*c* = 2.5 x 10^{-5} M) at 442 nm upon addition of 10 equiv. amounts of metal ions (*c* = 1.0 x 10^{-3} M) in DMSO: H_2O (1:9, v/v).

Change in emission of 1 in DMSO: H_2O (1:9, v/v).

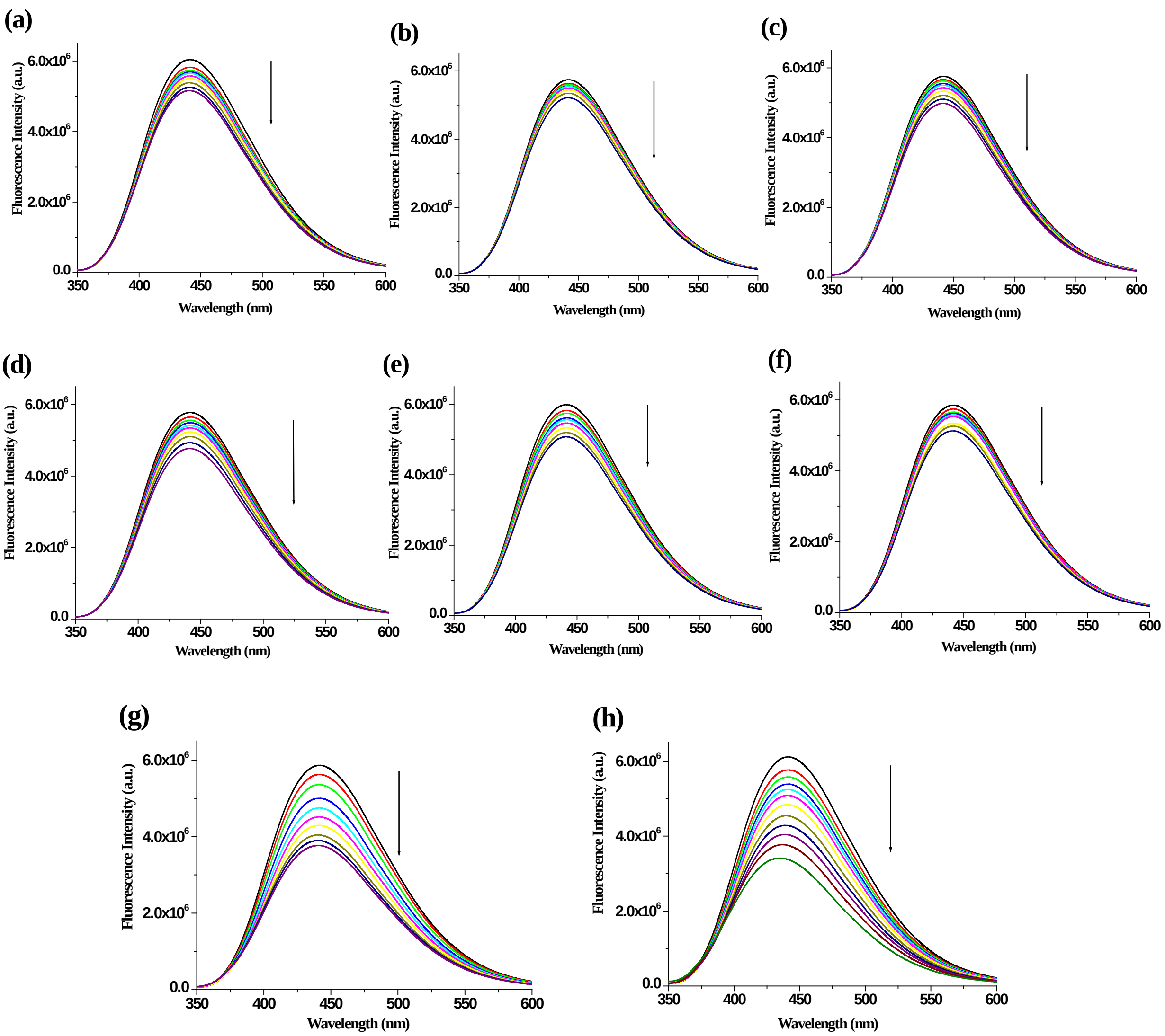

Fig. S16. Change in emission of **1** (c = 2.5 x 10^{-5} M) upon addition of 10 equiv. amount of (a) Pb^{2+}, (b) Mg^{2+}, (c) Co^{2+}, (d) Ni^{2+}, (e) Zn^{2+}, (f) Cd^{2+}, (g) Fe^{2+} and (h) Hg^{2+} (c = 1.0 x 10^{-3} M)) in DMSO: H_2O (1:9, v/v).

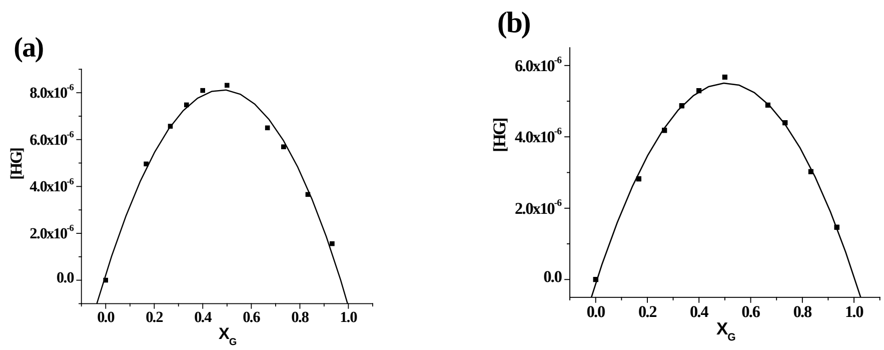

Fig. S17. Job plots of receptor **1** (c = 2.5 x 10^{-5} M) with (a) Ag^{+} and (b) Cu^{2+} from fluorescence.

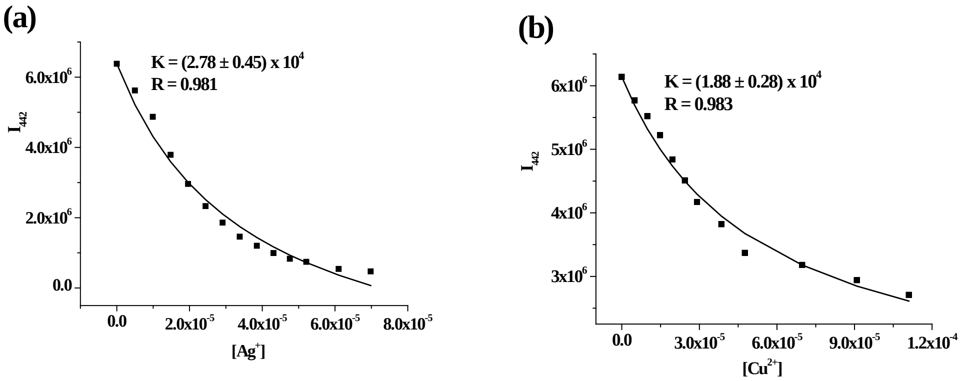

Fig. S18. Non liner binding constant curves for **1** (c = 2.5 x 10^{-5} M) with (a) Ag^+ and (b) Cu^{2+} (c = 1.0 x 10^{-3} M) in DMSO: H_2O (1:9, v/v) from fluorescence.

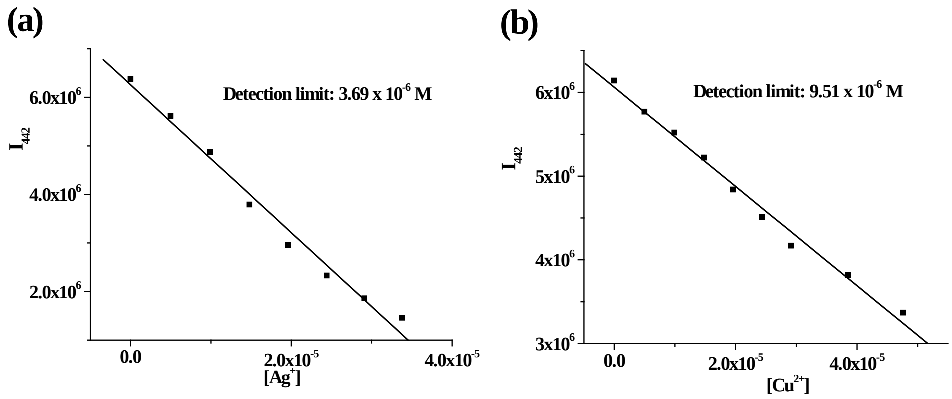

Fig. S19. Detection limits of **1** (c = 2.5 x 10^{-5} M) with (a) Ag^+ and (b) Cu^{2+} (c = 1.0 x 10^{-3} M) in DMSO: H_2O (1:9, v/v) from fluorescence.

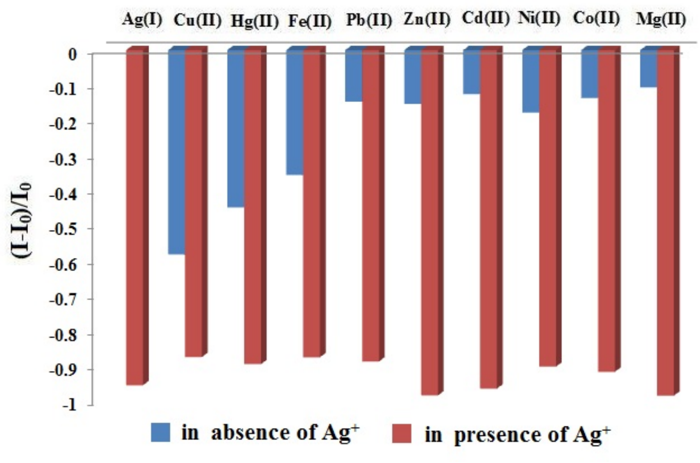

Fig. S20. Fluorescence response of **1** (c = 2.50 x 10^{-5} M) upon addition of 10 equiv. amounts of Ag^+ ions to the solution of **1** containing other metal ions in 10 equiv. amounts in DMSO: H_2O (1:9, v/v)**.**

Change in emission of 2 with metal ions

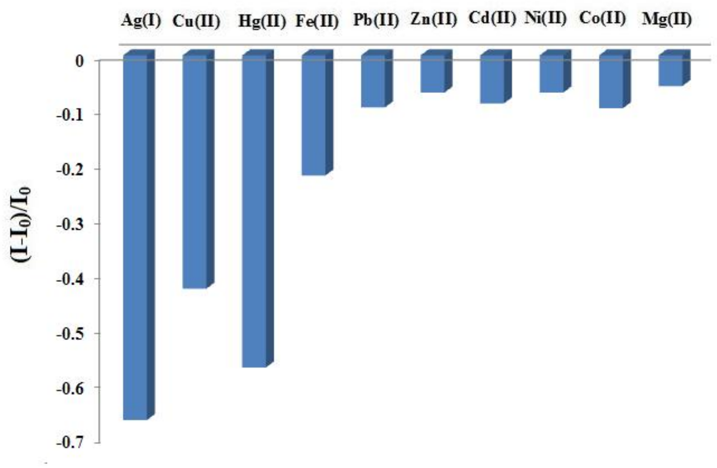

Fig. S21. Change in fluorescence ratio (λ_{ex} = 300 nm) of **2** (c = 2.5 x 10^{-5} M) at 382 nm upon addition of 20 equiv. amounts of metal ions (c = 1.0 x 10^{-3} M) in DMSO: H_2O (1:9, v/v).

Change in emission of 2 in DMSO: H_2O (1:9, v/v).

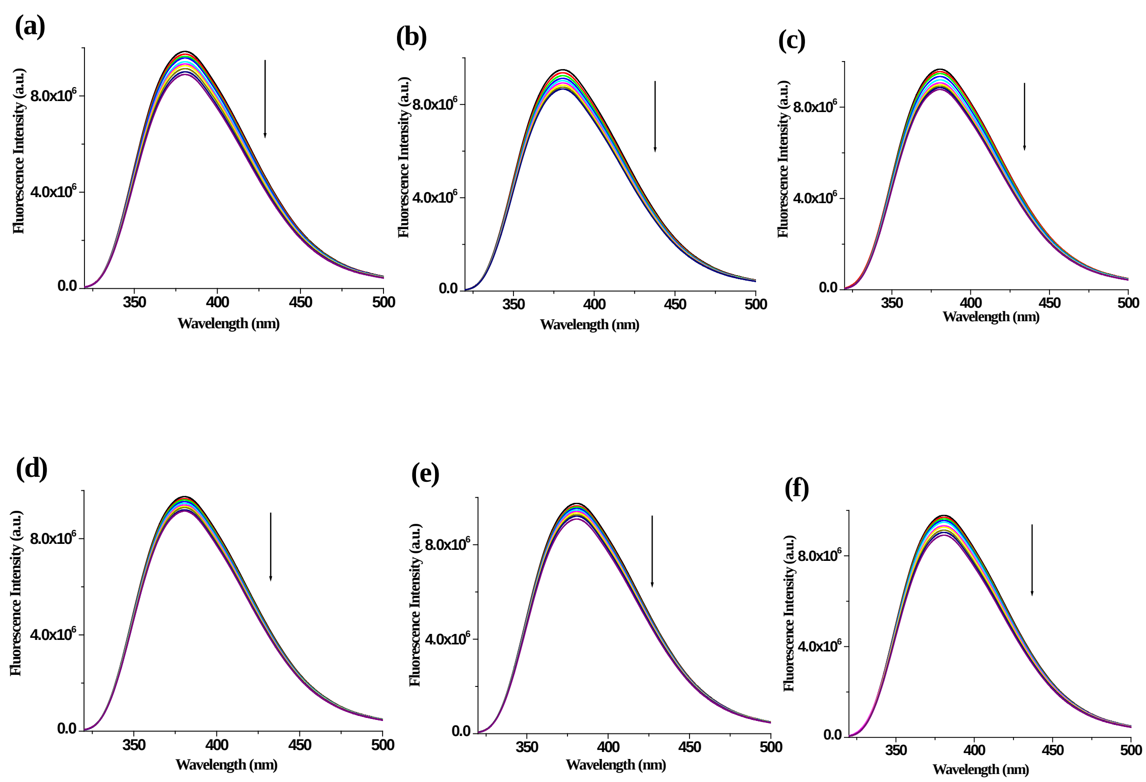

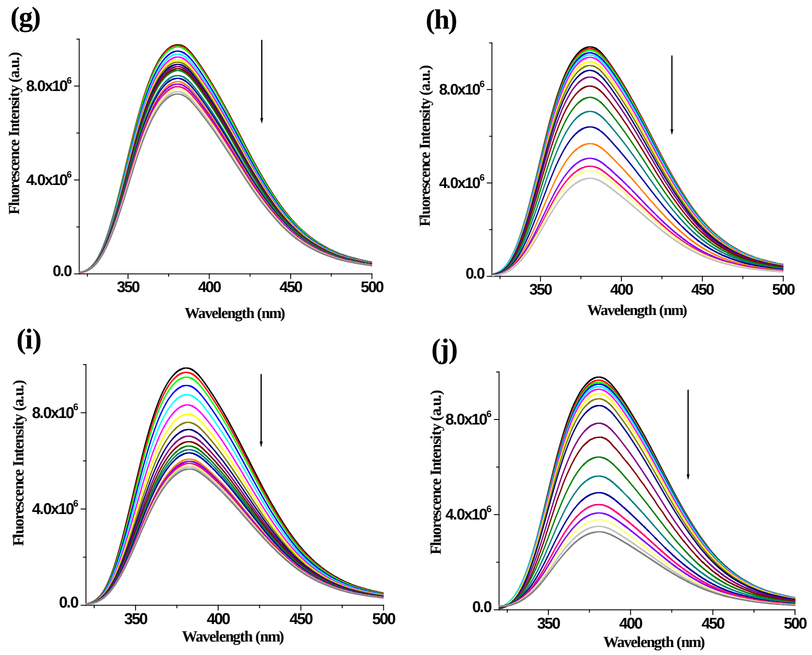

Fig. S22. Change in emission of **2** (c = 2.5 x 10^{-5} M) upon addition of 20 equiv. amount of (a) Pb^{2+}, (b) Mg^{2+}, (c) Co^{2+}, (d) Ni^{2+}, (e) Zn^{2+}, (f) Cd^{2+}, (g) Fe^{2+}, (h) Hg^{2+}, (i) Cu^{2+}, (j) Ag^{+} (c = 1.0 x 10^{-3} M)) in DMSO: H_2O (1:9, v/v).

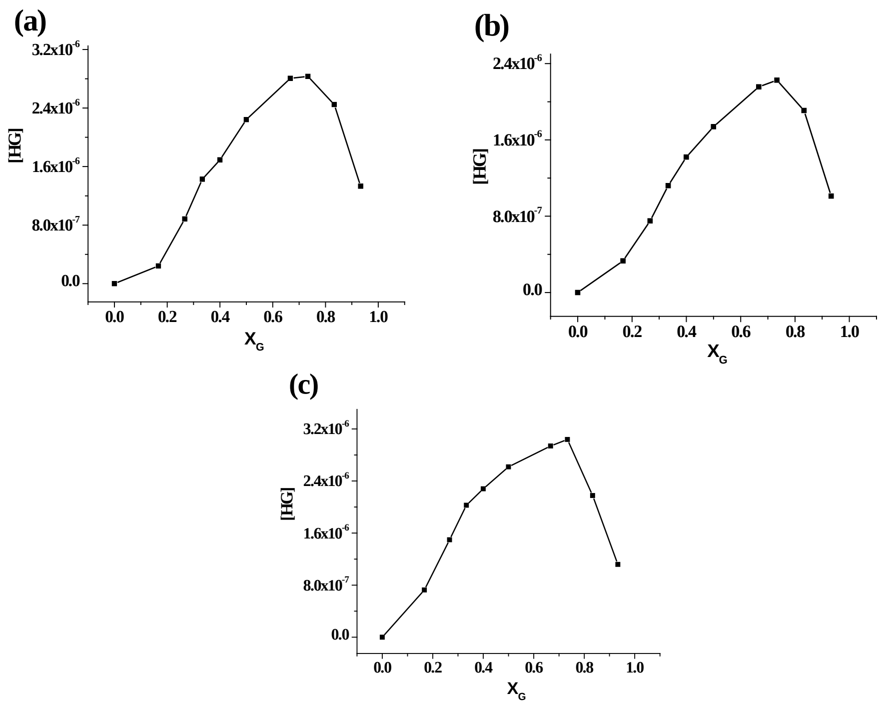

Fig. S23. Job plots of receptor **2** (c = 2.5 x 10^{-5} M) with (a) Ag^{2+}, (b) Cu^{2+} and (c) Hg^{2+} from fluorescence.

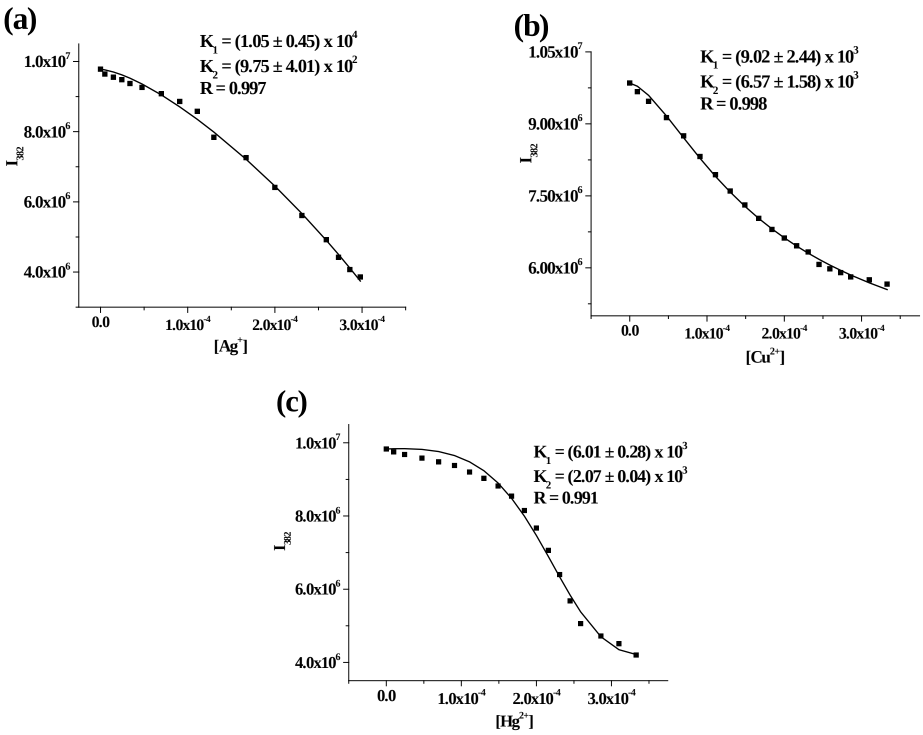

Fig. S24. Non liner binding constant curves for **2** (c = 2.5 x 10^{-5} M) with (a) Ag^{2+}, (b) Cu^{2+} and (c) Hg^{2+} (c = 1.0 x 10^{-3} M) in DMSO: H_2O (1:9, v/v) from fluorescence.

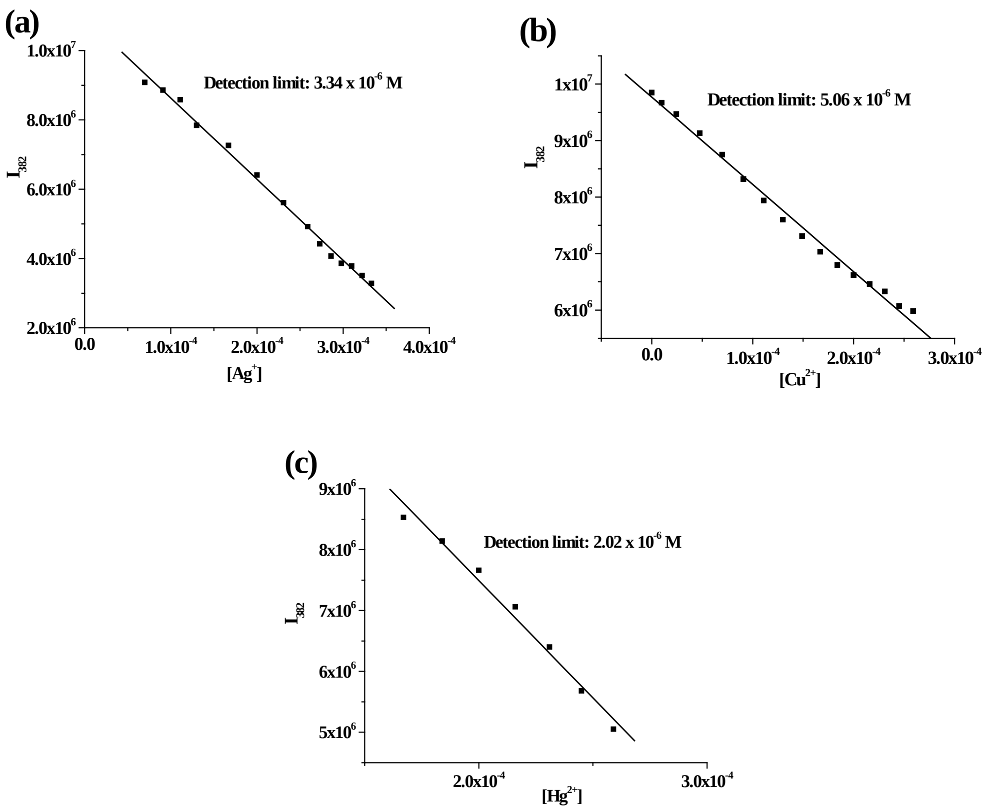

Fig. S25. Detection limits of **2** (c = 2.5 x 10^{-5} M) with (a) Ag^{2+}, (b) Cu^{2+} and (c) Hg^{2+} (c = 1.0 x 10^{-3} M) in DMSO: H_2O (1:9, v/v) from fluorescence.

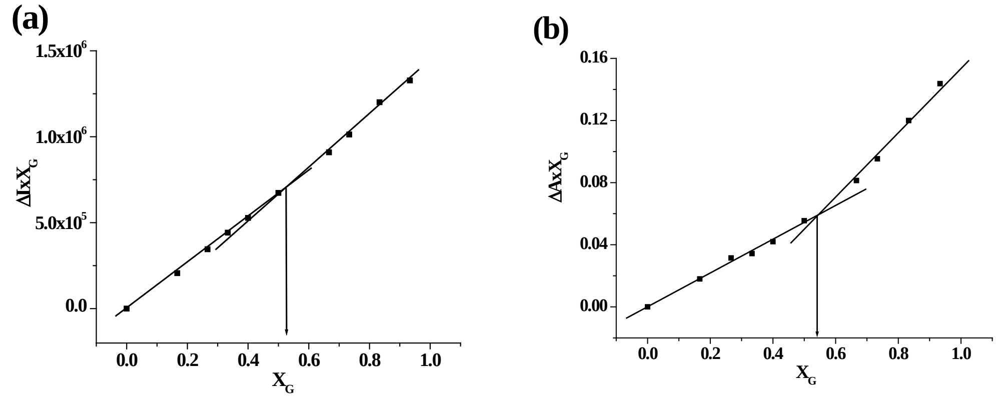

Fig. S26. Job plot of receptors **3** (c = 2.5 x 10^{-5} M) with Ag^+ from (a) fluorescence and (b) UV.

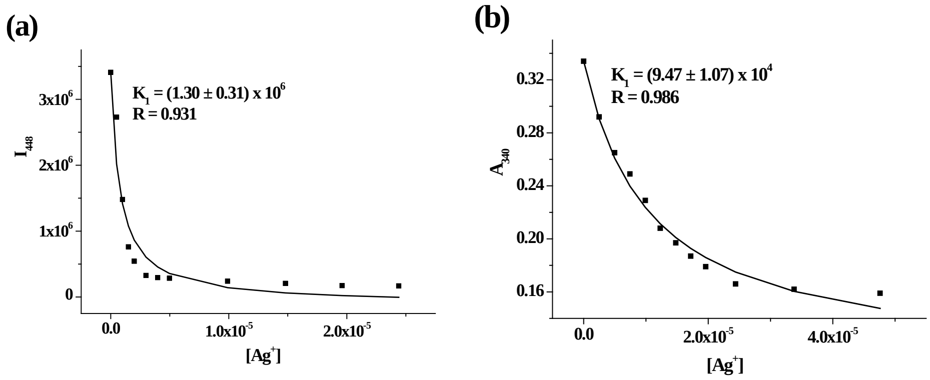

Fig. S27. Non liner binding constant curves for **3** (c = 2.5 x 10^{-5} M) with Ag^+ (c = 1.0 x 10^{-3} M) in DMSO: H_2O (1:9, v/v) from (a) fluorescence and (b) UV.

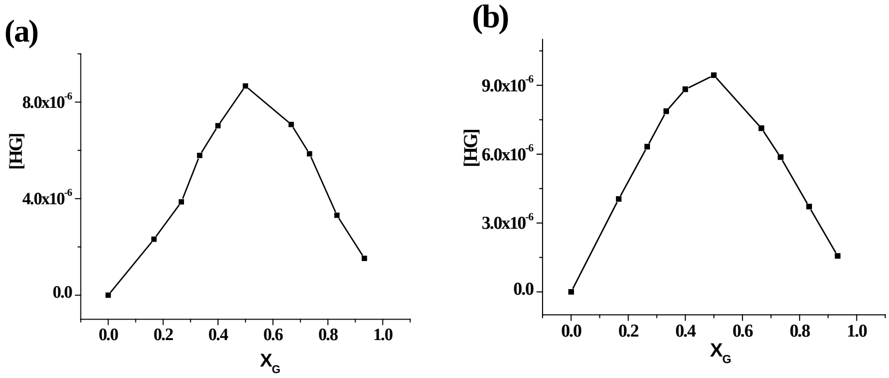

Fig. S28. Job plots of receptor **4** (c = 2.5 x 10^{-5} M) with Ag^+ from (a) fluorescence and (b) UV.

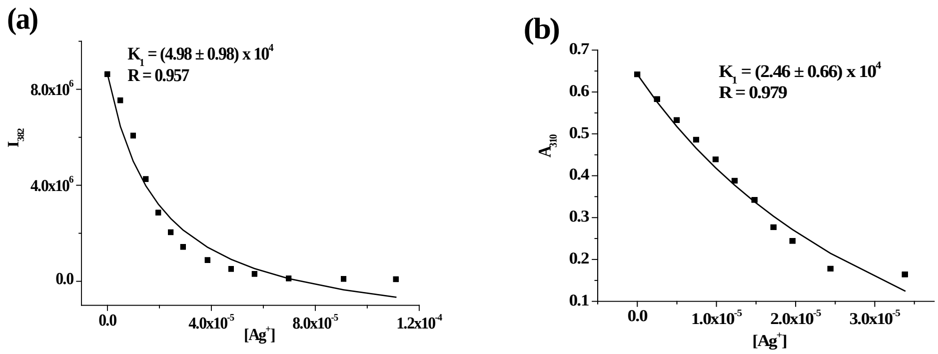

Fig. S29. Non liner binding constant curves for **4** (c = 2.5 x 10^{-5} M) with Ag^+ (c = 1.0 x 10^{-3} M) in DMSO: H_2O (1:9, v/v) from (a) fluorescence and (b) UV.

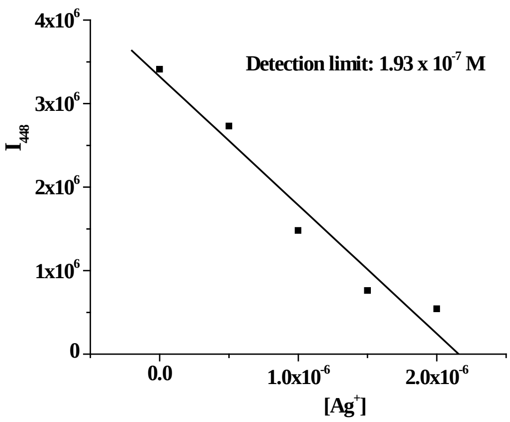

Fig. S30. Detection limit of **3** (c = 2.5 x 10^{-5} M) with Ag^+ (c = 1.0 x 10^{-3} M) in DMSO: H_2O (1:9, v/v) from fluorescence.

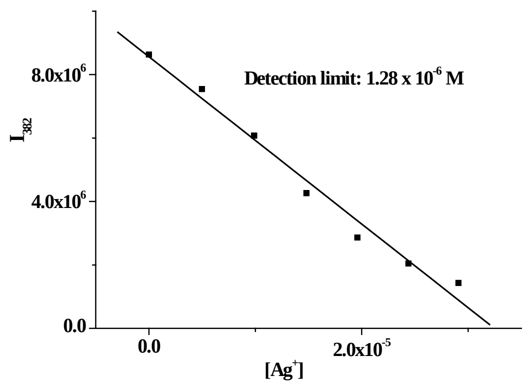

Fig. S31. Detection limit of **4** (c = 2.5 x 10^{-5} M) with Ag^+ (c = 1.0 x 10^{-3} M) in DMSO: H_2O (1:9, v/v) from fluorescence.

Change in absorbance of 1 in DMSO: H_2O (1:9, v/v).

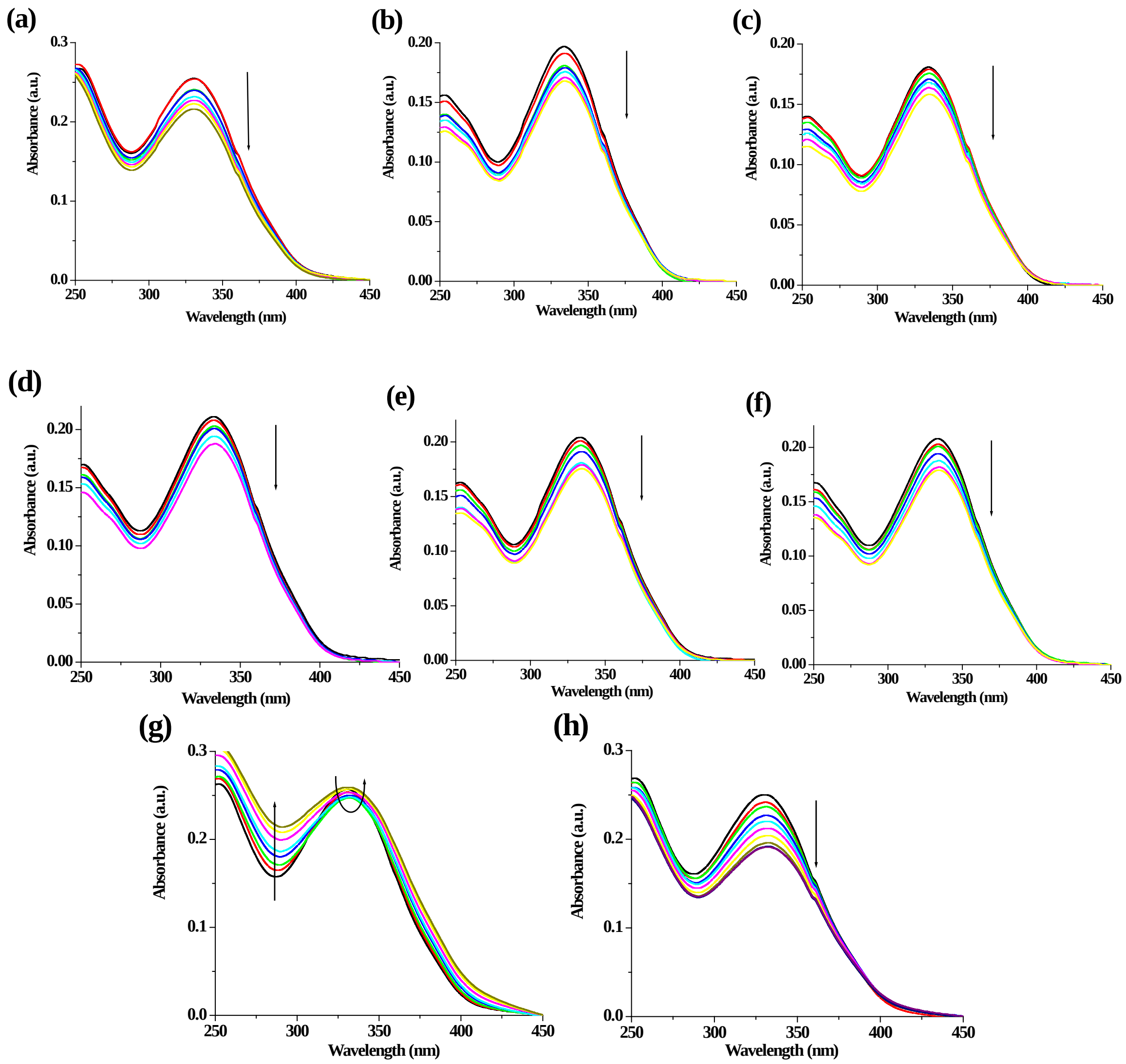

Fig. S32. Change in absorbance of **1** (c = 2.5 x 10^{-5} M) upon addition of 6 equiv. amount of (a) Pb^{2+}, (b) Mg^{2+}, (c) Co^{2+}, (d) Ni^{2+}, (e) Zn^{2+}, (f) Cd^{2+}, (g) Fe^{2+}, (h) Hg^{2+} (c = 1.0 x 10^{-3} M) in DMSO: H_2O (1:9, v/v).

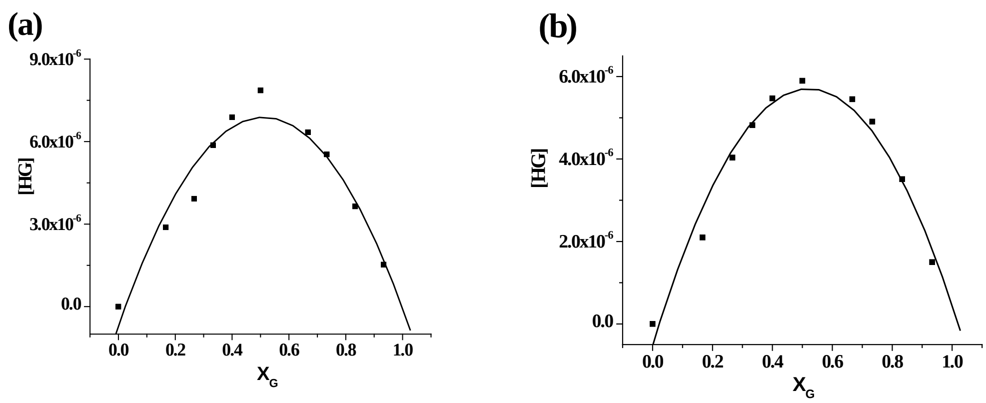

Fig. S33. Job plots of receptor **1** (c = 2.5 x 10^{-5} M) with (a) Ag^{+} and (b) Cu^{2+} from UV.

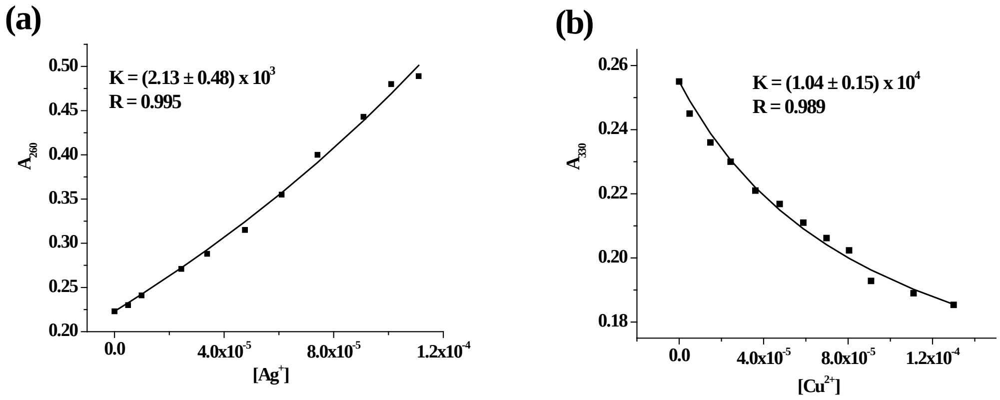

Fig. S34. Non liner binding constant curve for **1** (c = 2.5 x 10^{-5} M) with (a) Ag^+ and (b) Cu^{2+} (c = 1.0 x 10^{-3} M) in DMSO: H_2O (1:9, v/v) from UV.

Change in absorbance of 2 in DMSO: H_2O (1:9, v/v).

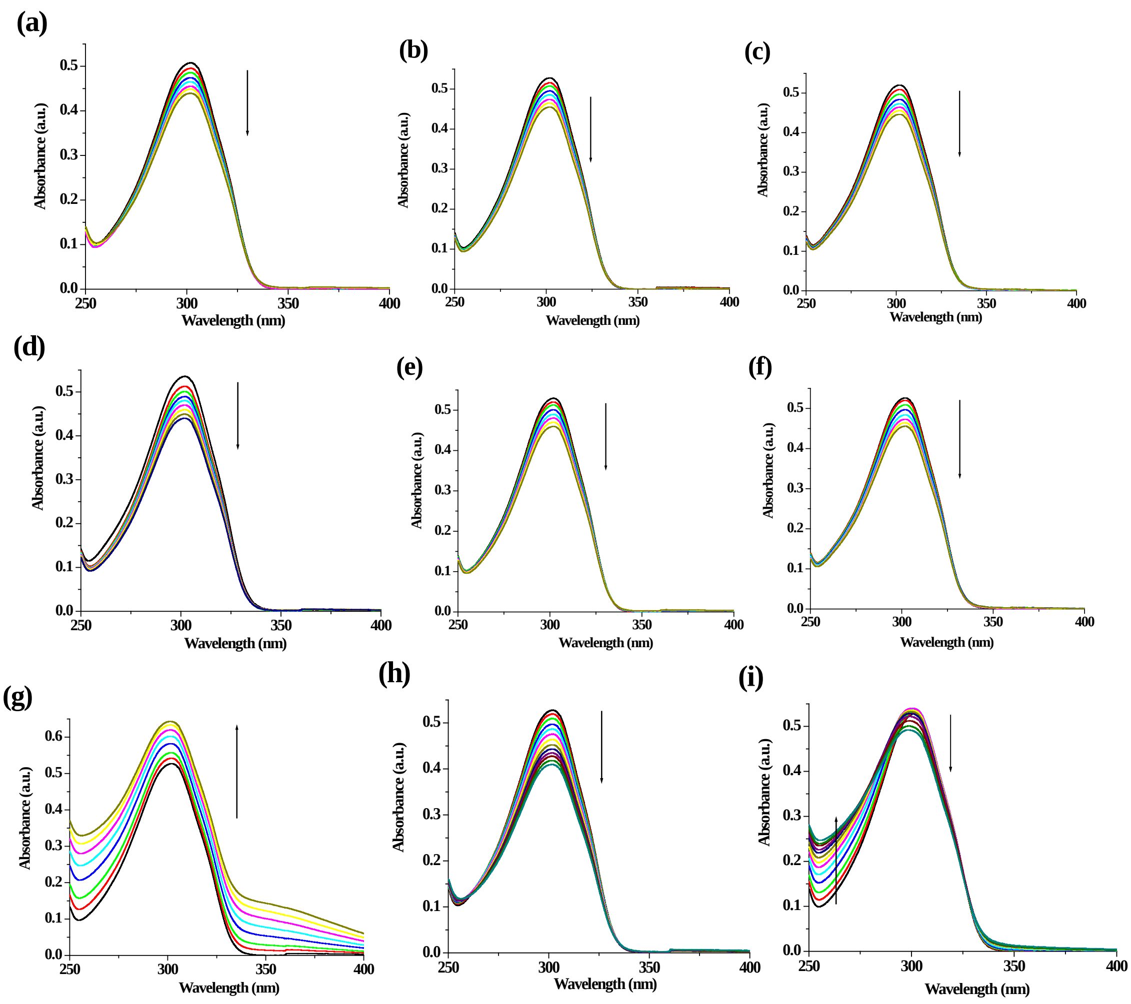

(j)

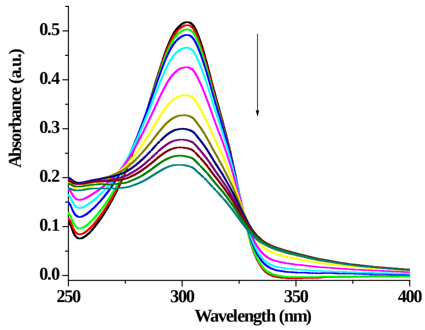

Fig. S35. Change in absorbance of **2** (c = 2.5 x 10^{-5} M) upon addition of 10 equiv. amount of (a) Pb^{2+}, (b) Mg^{2+}, (c) Co^{2+}, (d) Ni^{2+}, (e) Zn^{2+}, (f) Cd^{2+}, (g) Fe^{2+}, (h) Hg^{2+}, (i) Cu^{2+}, (j) Ag^{+} (c = 1.0 x 10^{-3} M) in DMSO: H_2O (1:9, v/v).

(a)

(b)

(c)

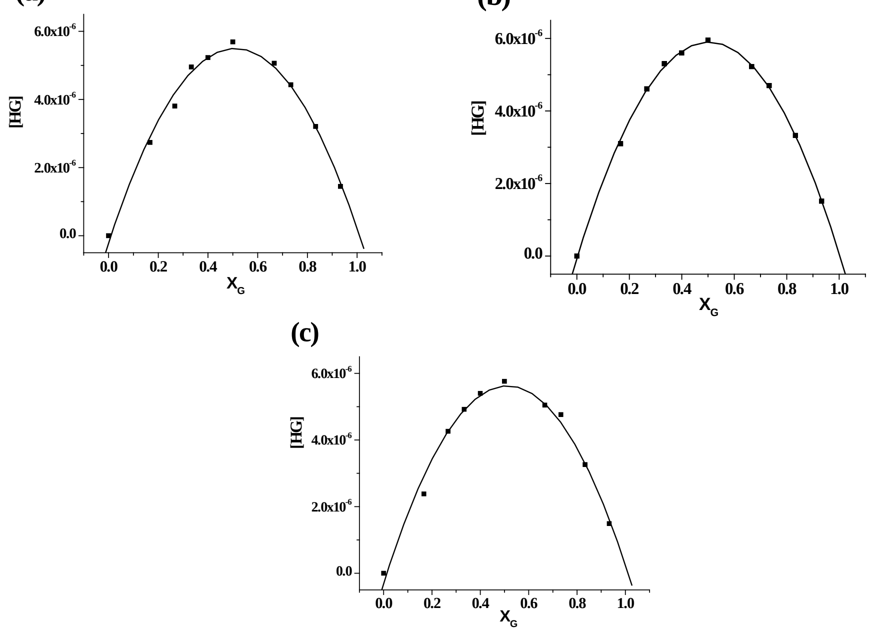

Fig. S36. Job plots of receptor **2** (c = 2.5 x 10^{-5} M) with (a) Ag^{+}, (b) Cu^{2+} and (c) Hg^{2+} from UV.

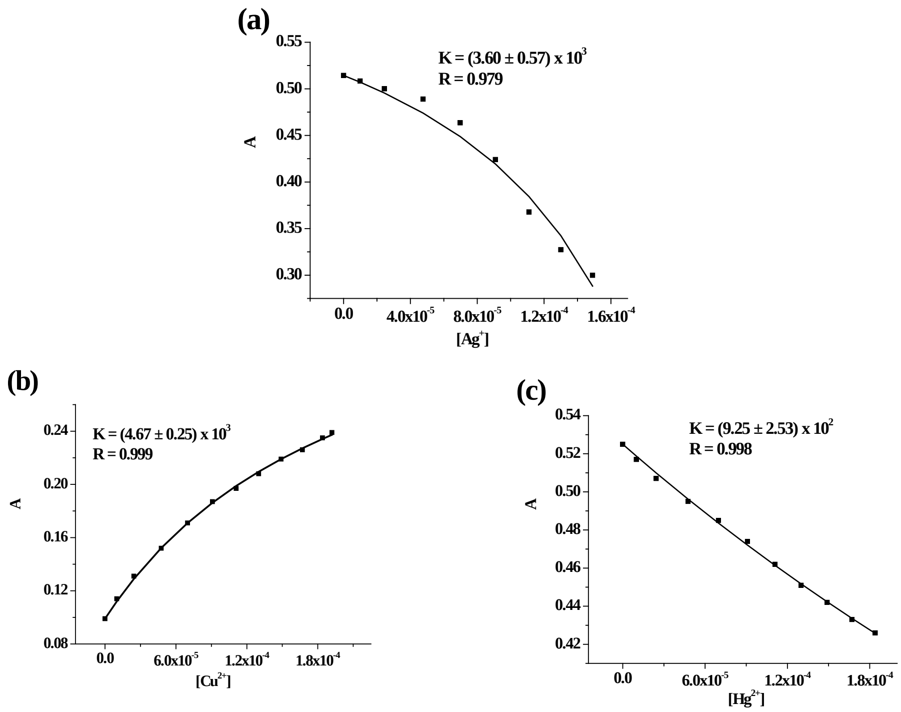

Fig. S37. Non liner binding constant curves for **2** (c = 2.5 x 10^{-5} M) with (a) Ag^{2+}, (b) Cu^{2+} and (c) Hg^{2+} (c = 1.0 x 10^{-3} M) in DMSO: H_2O (1:9, v/v) from UV.

Table S2. Non liner binding constant data for **1-4** (c = 2.5 x 10^{-5} M) with respective metal ions (c = 1.0 x 10^{-3} M) in DMSO: H_2O (1:9, v/v).

Metal- ligand complex	**Binding constant values (M^{-1})**	
	From florescence titration data	**From UV titration data**
1 - Ag^+	K = (2.78 ± 0.45) x 10^4	K = (2.13 ± 0.48) x 10^3
1 - Cu^{2+}	K = (1.88 ± 0.28) x 10^4	K = (1.04 ± 0.15) x 10^4
2 - Ag^+	K_1 = (1.05 ± 0.15) x 10^4	K = (3.60 ± 0.57) x 10^3
	K_2 = (9.75 ± 4.01) x 10^2	
2 - Cu^{2+}	K_1 = (9.02 ± 2.44) x 10^3	K = (4.67 ± 0.25) x 10^3
	K_2 = (6.57 ± 1.58) x 10^3	
2 - Hg^+	K_1 = (6.01 ± 0.28) x 10^3	K = (9.25 ± 2.53) x 10^3
	K_2 = (2.07 ± 0.04) x 10^3	
3 - Ag^+	K = (1.30 ± 0.31) x 10^6	K = (9.47 ± 1.07) x 10^4
4 - Ag^+	K = (4.98 ± 0.98) x 10^4	K = (2.46 ± 0.66) x 10^4

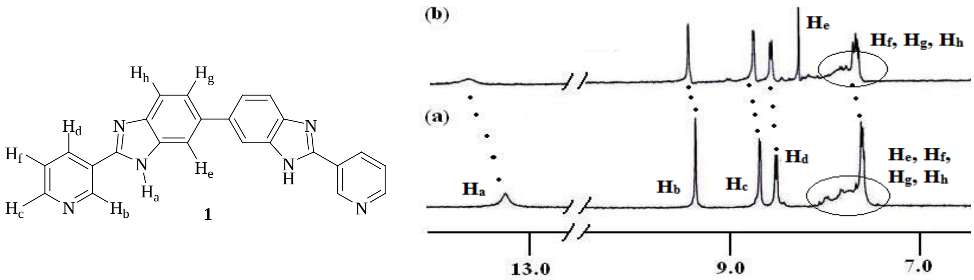

Fig. S38. ^{1}H NMR (400 MHz, d_6-DMSO) of (a) compound **1** (c = 1.50 x 10^{-2} M) and (b) **1** with equiv. amount of $AgClO_4$.

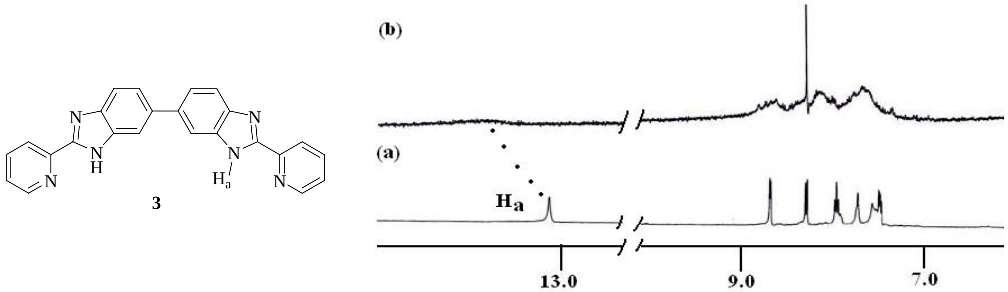

Fig. S39. ^{1}H NMR (400 MHz, d_6-DMSO) of (a) compound **3** (c = 1.07 x 10^{-2} M) and (b) **3** with equiv. amount of $AgClO_4$.

Table S3: List of metal ion responsive pyridine tied benzimidazoles as supramolecular gelators

Structure	Solvent	Metal ion (phase transformation)	Ref.
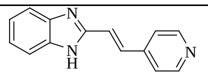	MeOH	Ag^{+} (Sol to gel)	*Chem. Commun*. 2013, 49, 4181
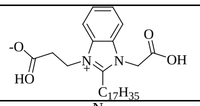	MeOH:H_2O (1:1, v/v)	Ag^{+} (Sol to gel)	*Supramol. Chem*. 2014, 26, 39
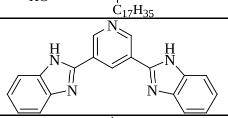	MeOH	Cu^{2+}, Cd^{2+} (Sol to gel)	*Chem. Mater*., 2012, 24, 1165
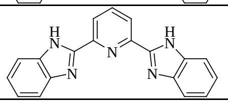	MeOH	Cu^{2+} (Sol to gel)	*CrystEngComm*, 2013, 15, 9769
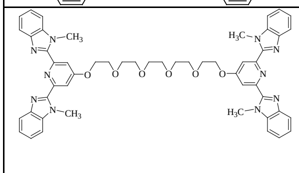	CH_3CN	Co^{2+}, Zn^{2+}, La^{3+}, Eu^{3+} (Sol to gel)	*J. Am. Chem. Soc.*, 2003, 125, 13922
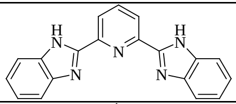	DMF	Zn^{2+}, Ni^{2+} (Sol to gel)	*J Porous Mater, 2016, 23, 663*
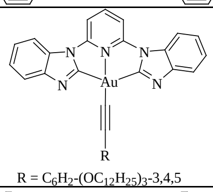 R = C_6H_2-$(OC_{12}H_{25})_3$-3,4,5	$CHCl_3$	Sol to gel	*Chem. Eur. J.*, 2014, 20, 9930
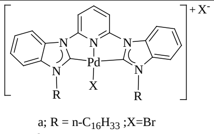 a; R = n-$C_{16}H_{33}$;X=Br b;R = n-$C_{16}H_{33}$;X=I	CH_3CN	Sol to gel	*Chem. Eur. J.*, 2009, 15, 1853

[1]H NMR (d_6-DMSO, 400 MHz)

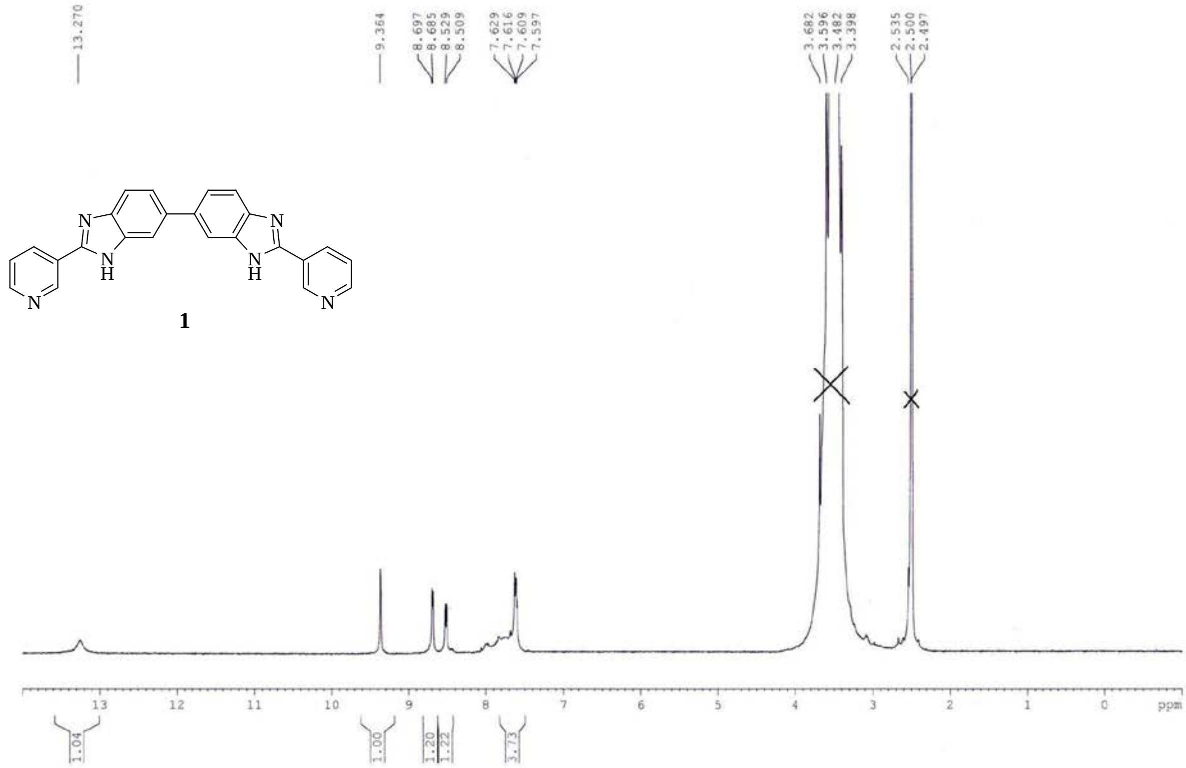

^{13}C NMR (d_6-DMSO, 100 MHz)

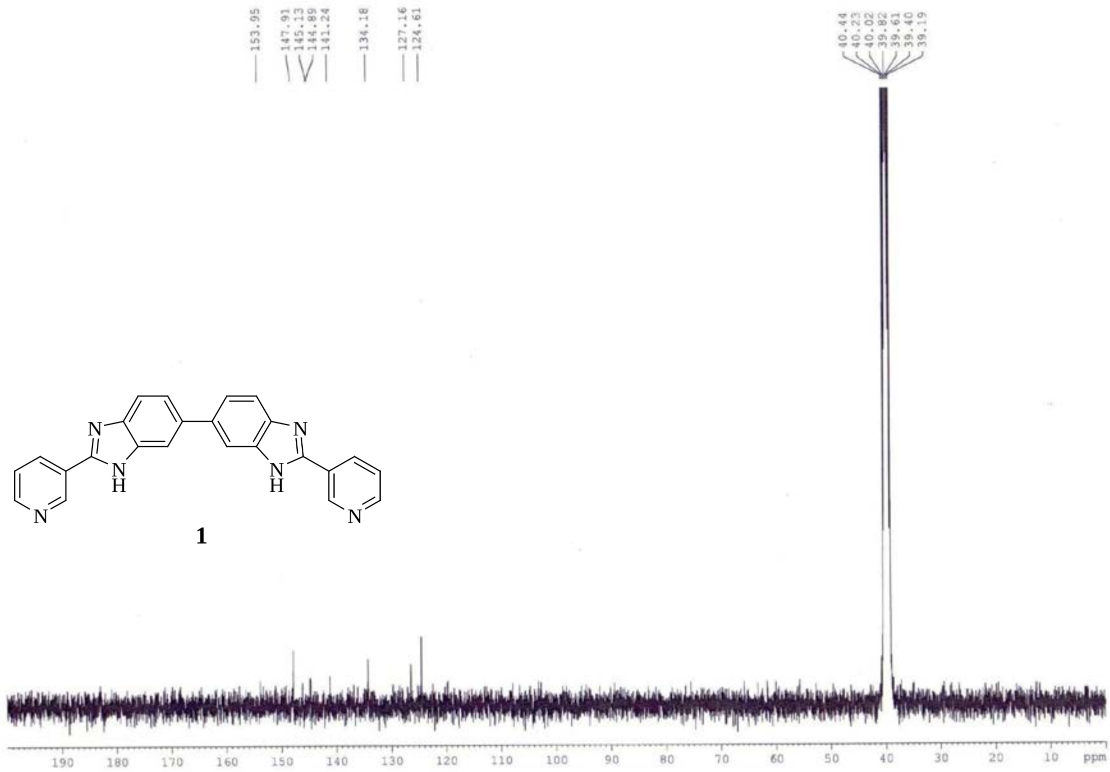

1

Mass spectrum of 1.

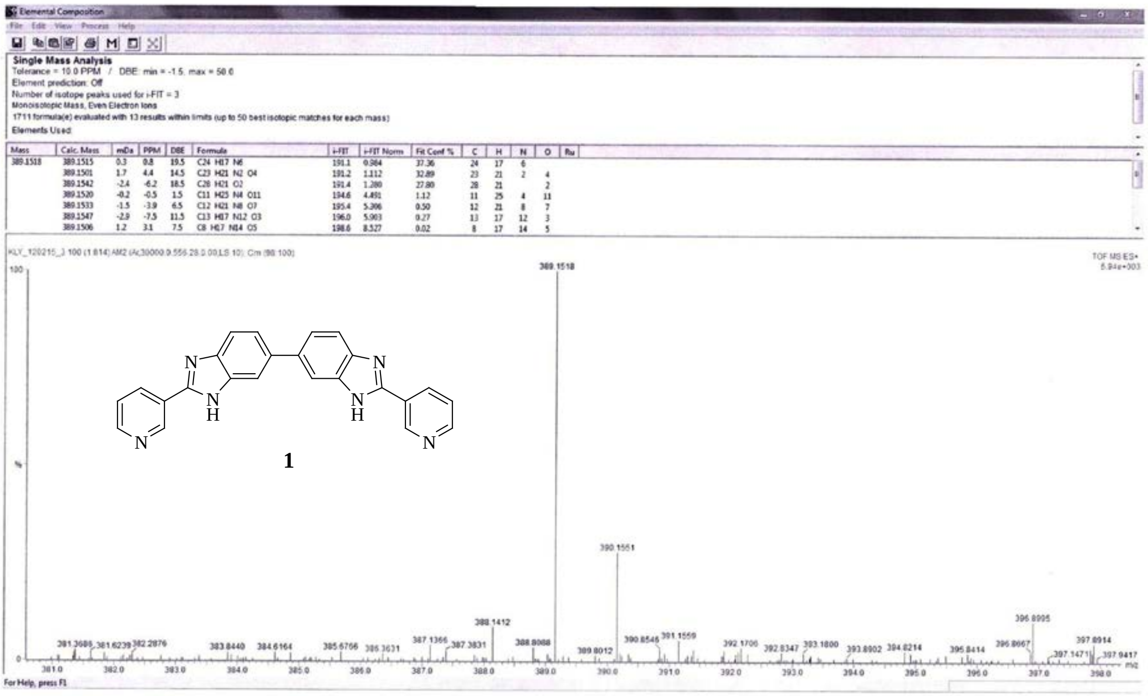

^{1}H NMR (d_6-DMSO, 400 MHz)

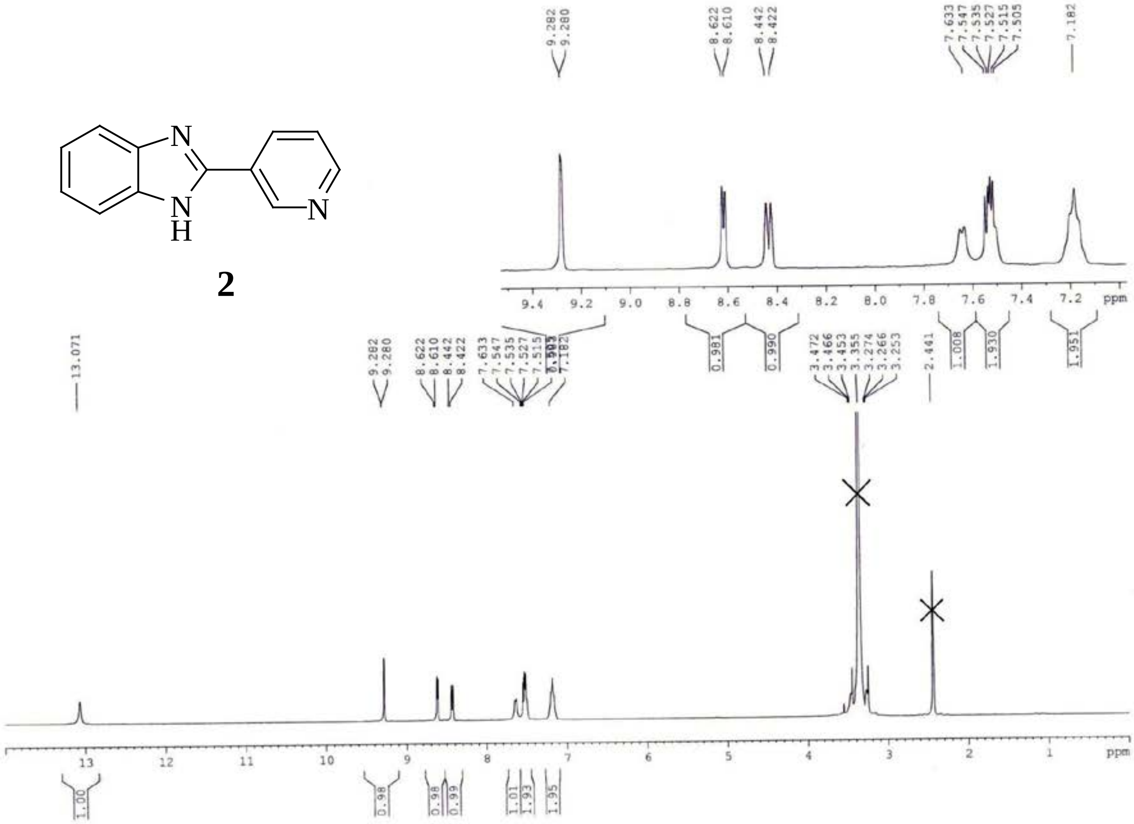

2

^{13}C NMR (d_6-DMSO, 100 MHz)

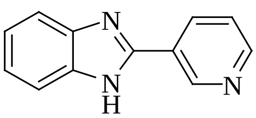

2

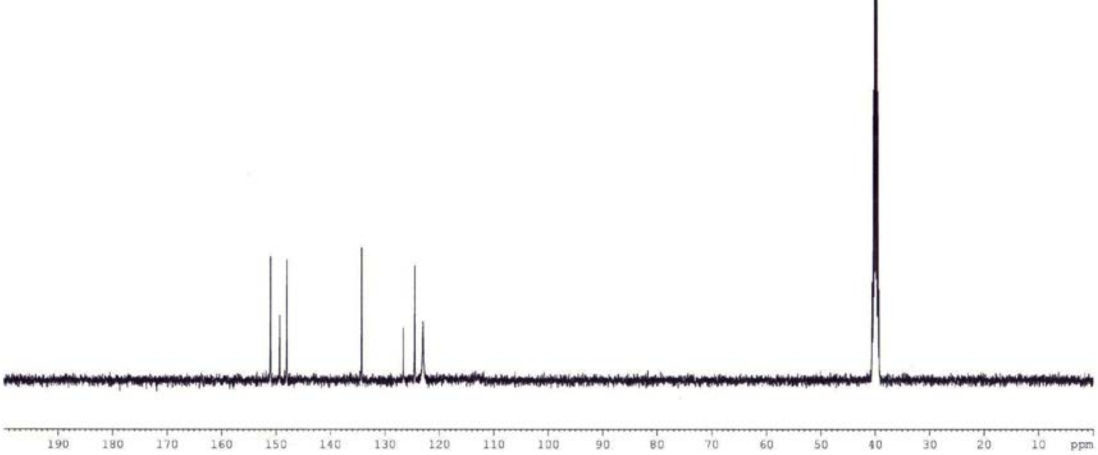

Mass spectrum of 2.

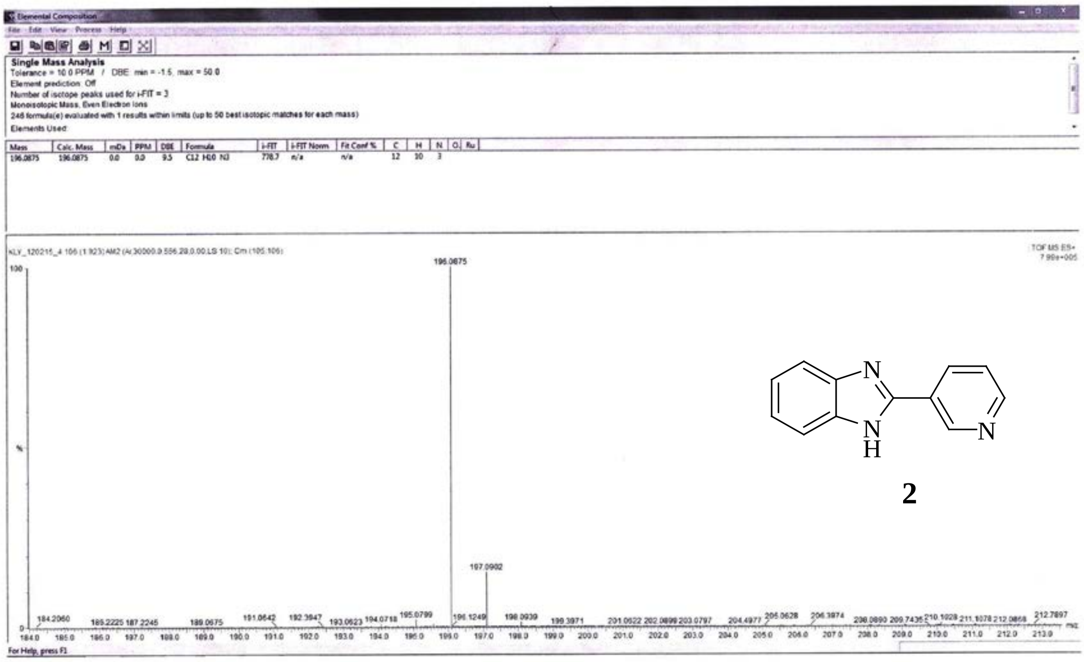

2

^{1}H NMR (d_6-DMSO, 400 MHz)

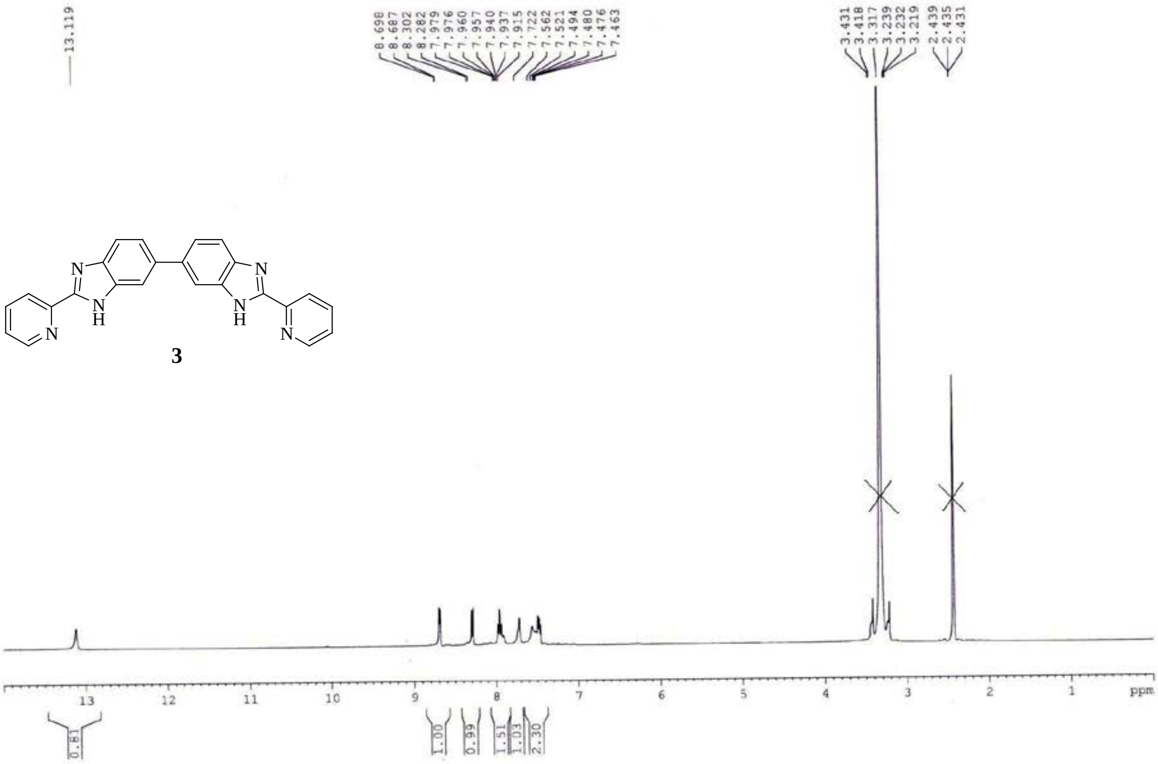
3

^{13}C NMR (d_6-DMSO, 100 MHz)

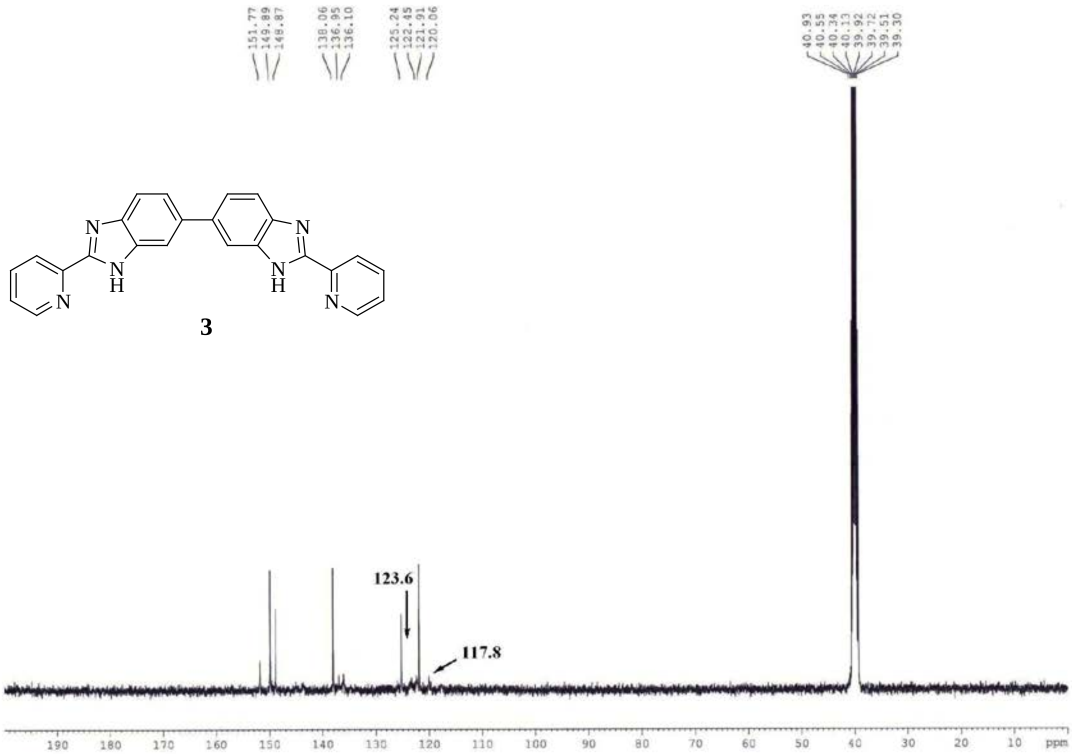

Mass spectrum of 3.

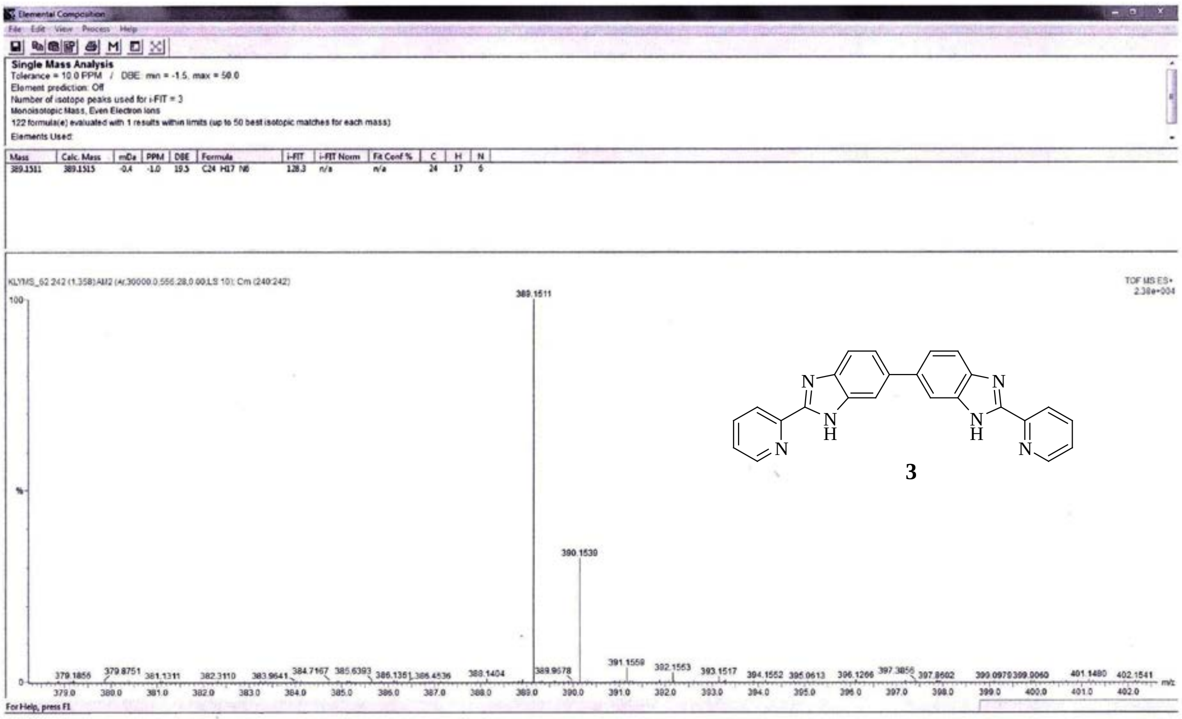

[1]H NMR (CDCl$_3$, 400 MHz)

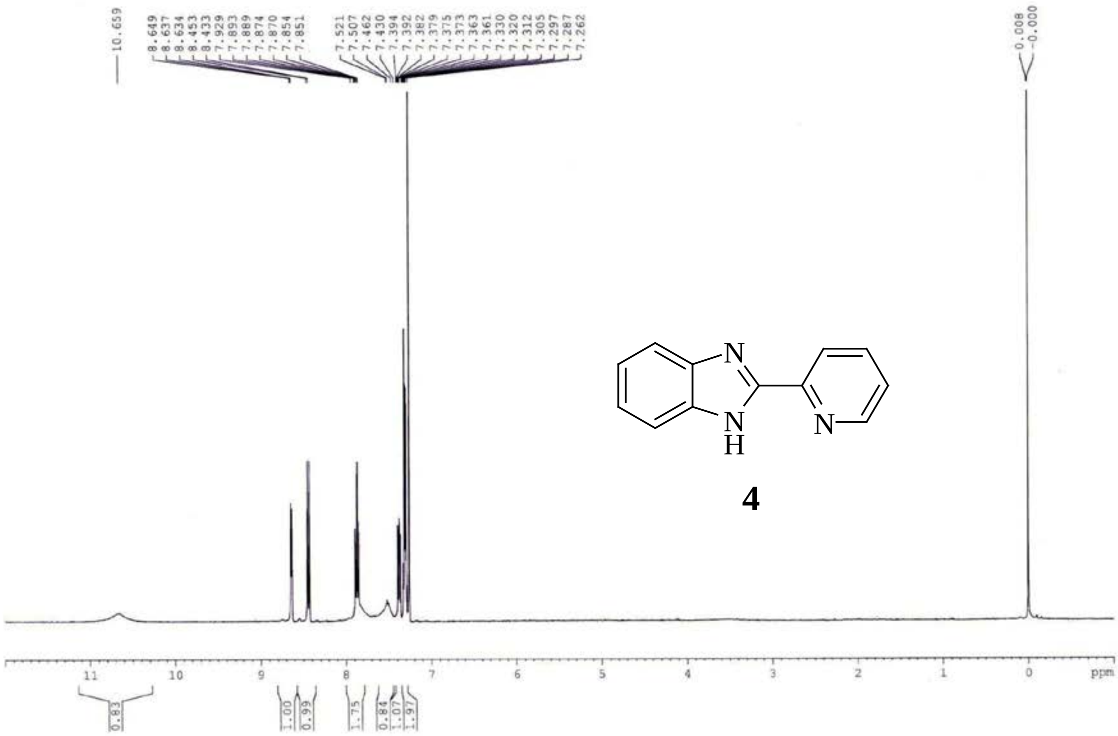

4

[13]C NMR (CDCl3, 100 MHz)

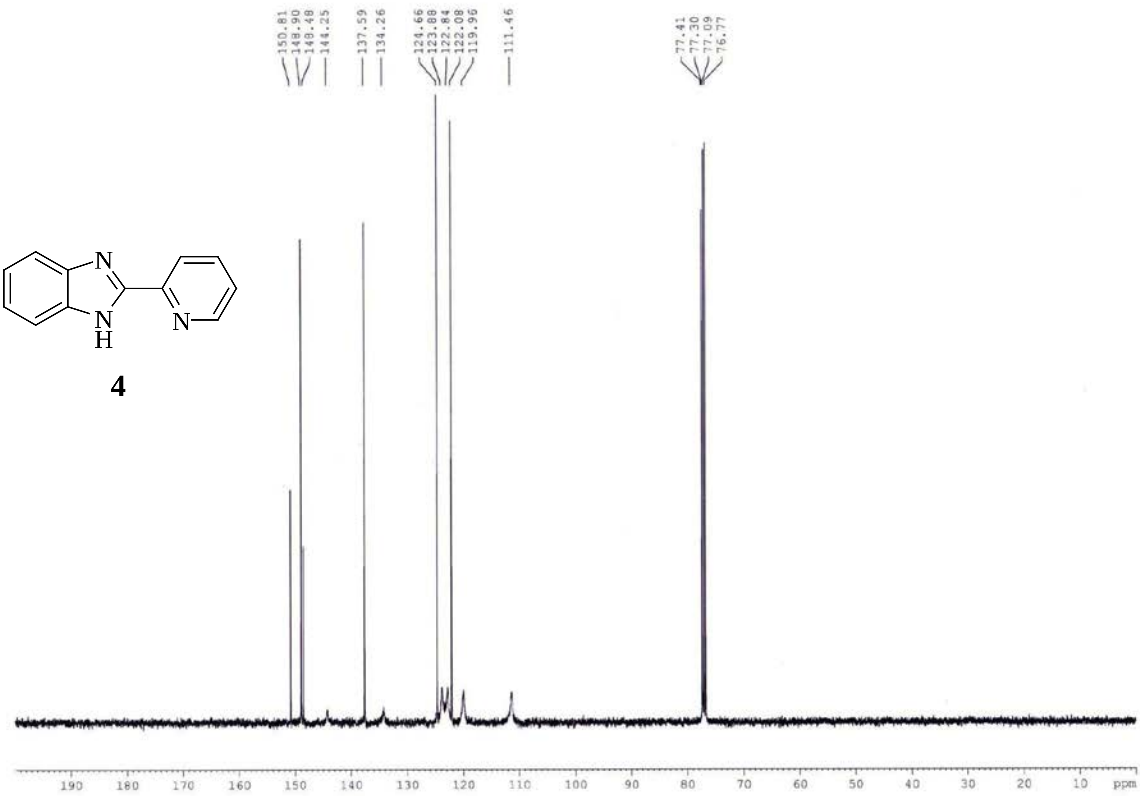

Mass spectrum of 4.

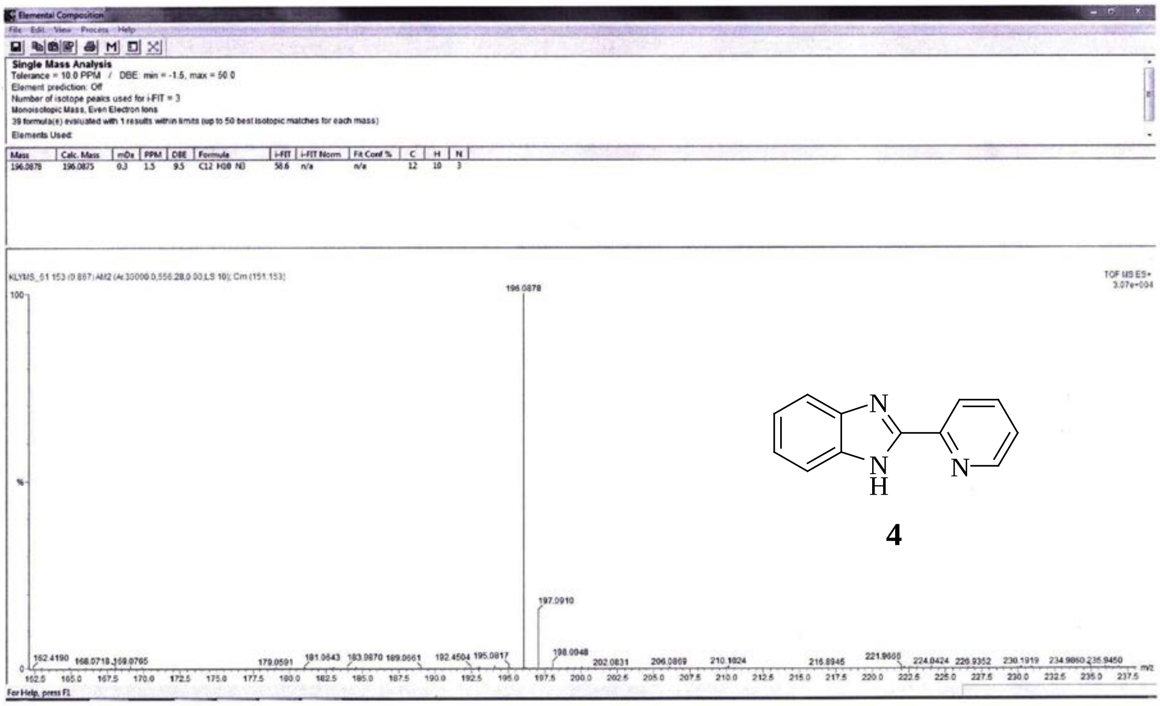

4

^{1}H NMR (d_6-DMSO, 400 MHz)

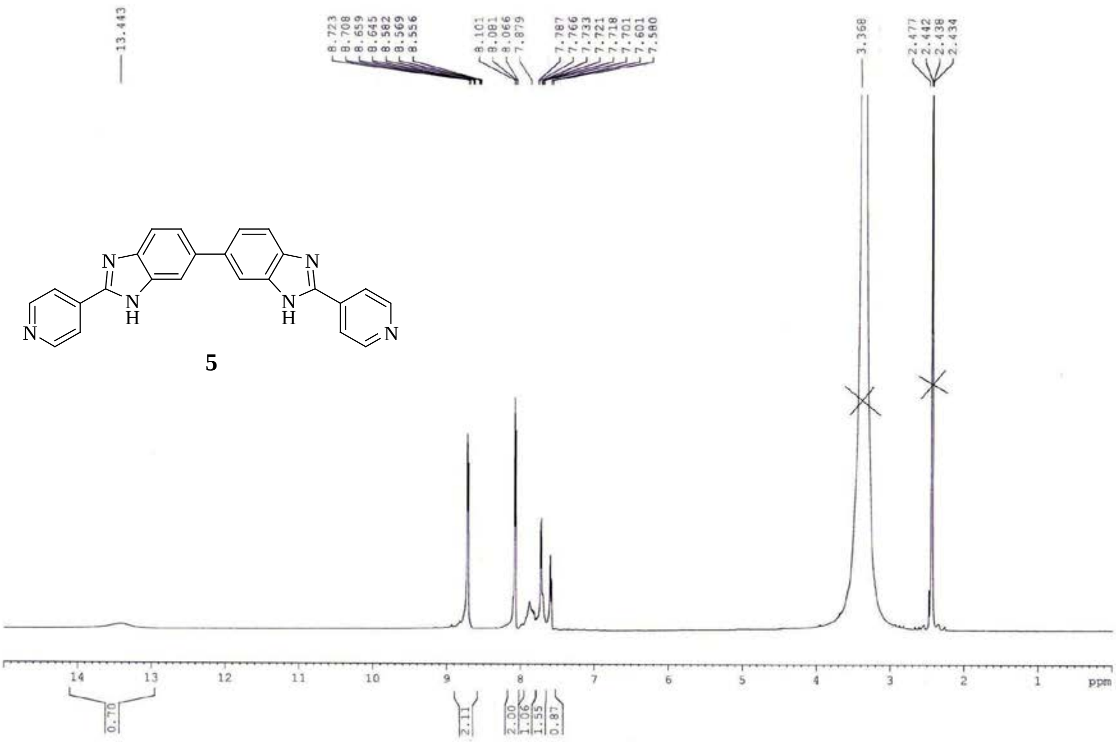

5

^{13}C NMR (d_6-DMSO, 100 MHz)

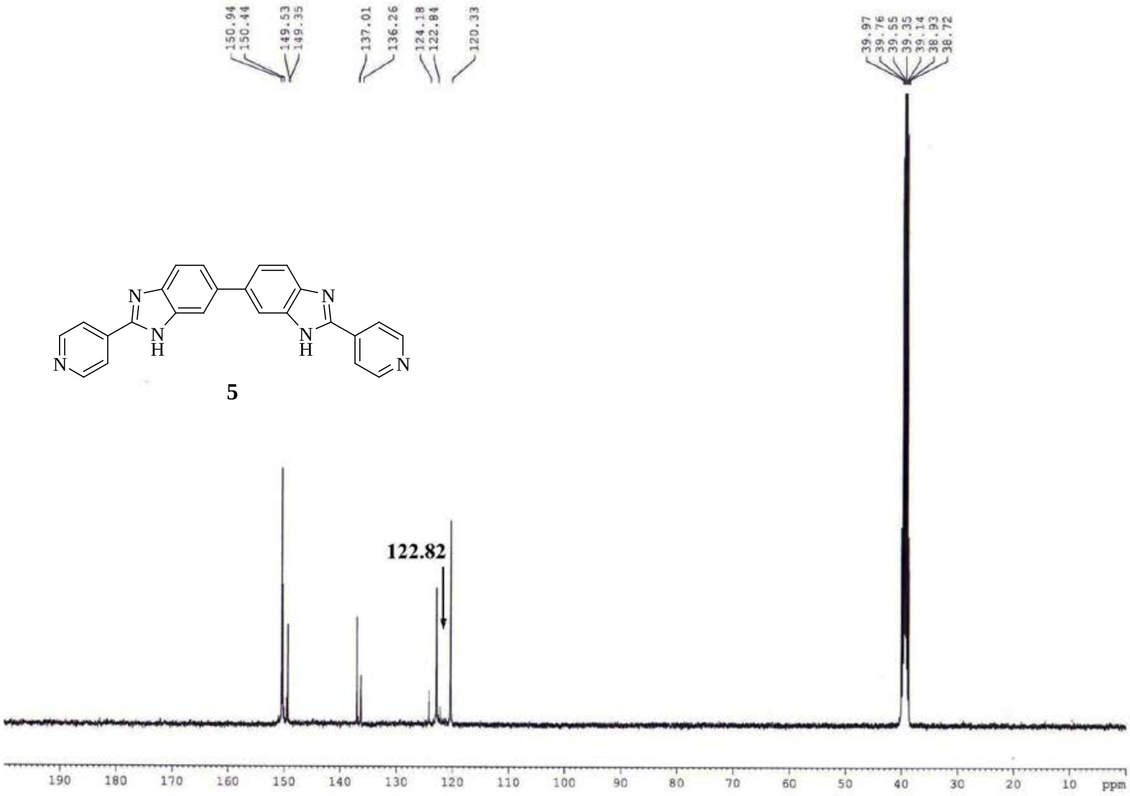

5

Mass spectrum of 5.

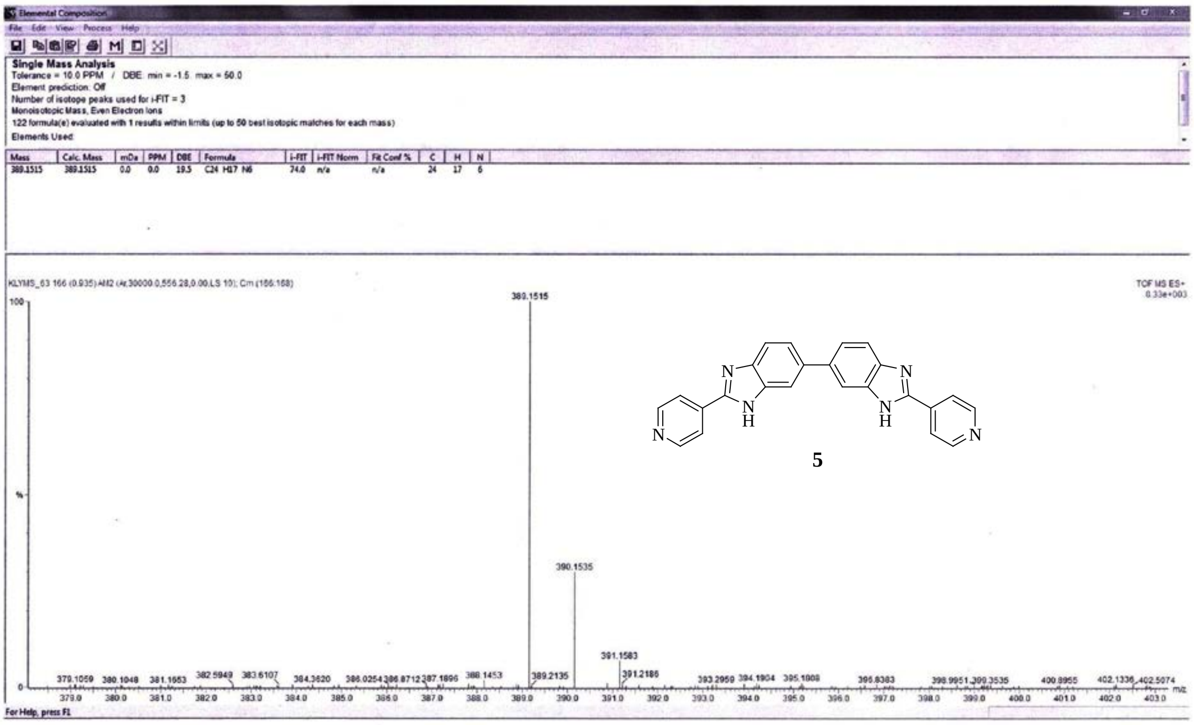

^{1}H NMR (d_6-DMSO, 400 MHz)

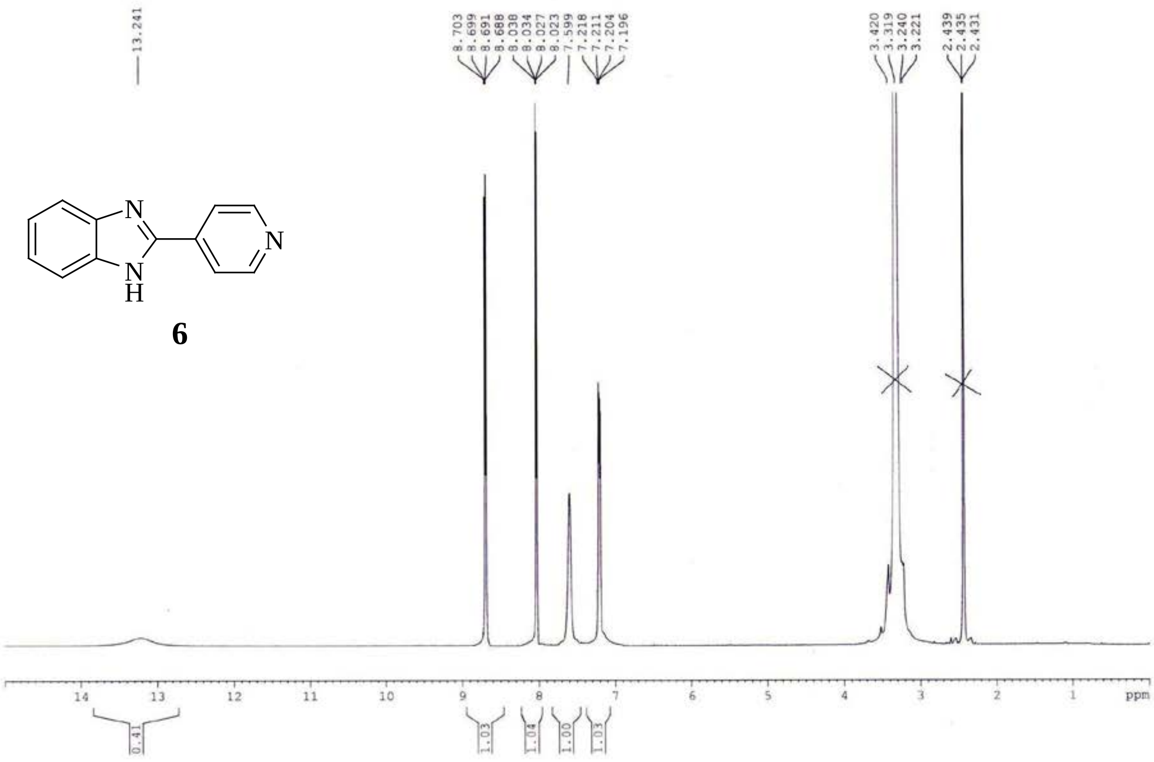

6

^{13}C NMR (d_6-DMSO, 100 MHz)

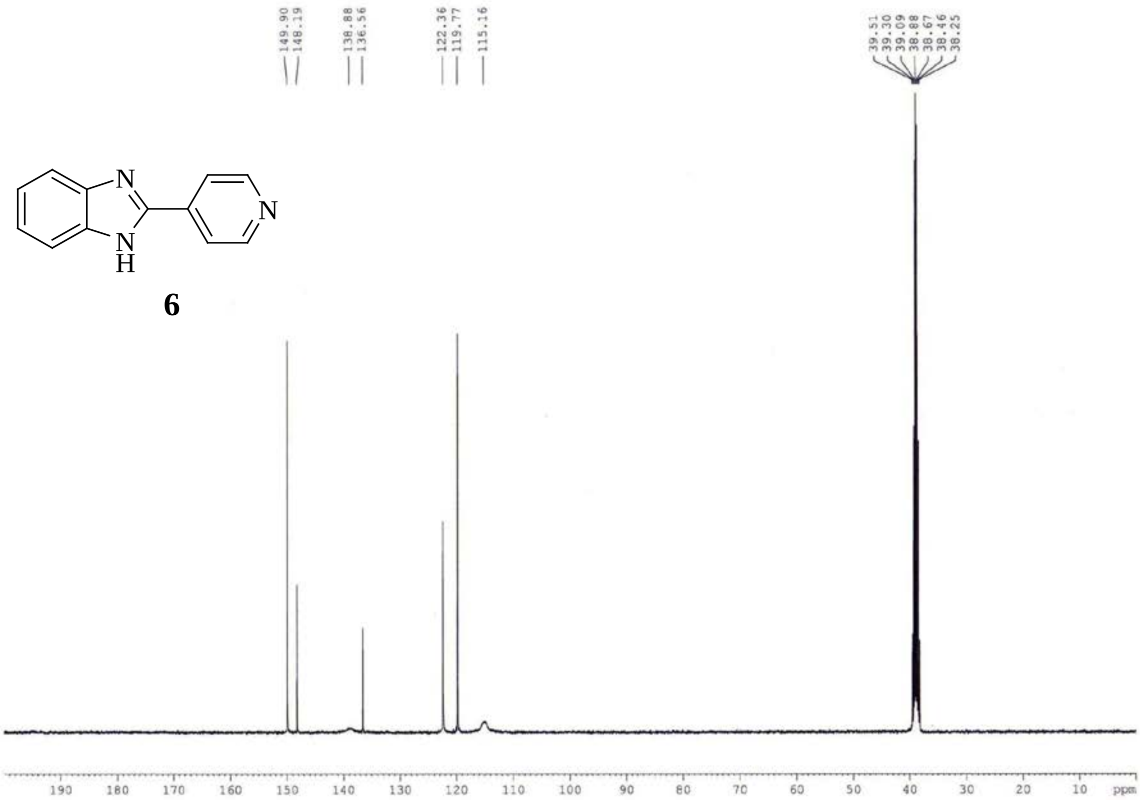

Mass spectrum of 6.